A Phosphorylation Site Regulates Sorting of the Vesicular Acetylcholine Transporter to Dense Core Vesicles

David E. Krantz,[‡§] Clarissa Waites,[*] Viola Oorschot,[¶] Yongjian Liu,[‡] Rachel I. Wilson,[‖] Philip K. Tan,[‡] Judith Klumperman,[¶] and Robert H. Edwards[*‡‖]

[*]Graduate Programs in Neuroscience, Cell Biology, and Biomedical Sciences, and [‡]Department of Neurology, [§]Department of Psychiatry, and [‖]Department of Physiology, University of California at San Francisco School of Medicine, San Francisco, California 94143-0435; and [¶]Department of Cell Biology, University Medical Center and Institute of Biomembranes, Utrecht University, 3584 CX Utrecht, The Netherlands

Abstract. Vesicular transport proteins package classical neurotransmitters for regulated exocytotic release, and localize to at least two distinct types of secretory vesicles. In PC12 cells, the vesicular acetylcholine transporter (VAChT) localizes preferentially to synaptic-like microvesicles (SLMVs), whereas the closely related vesicular monoamine transporters (VMATs) localize preferentially to large dense core vesicles (LDCVs). VAChT and the VMATs contain COOH-terminal, cytoplasmic dileucine motifs required for internalization from the plasma membrane. We now show that VAChT undergoes regulated phosphorylation by protein kinase C on a serine (Ser-480) five residues upstream of the dileucine motif. Replacement of Ser-480 by glutamate, to mimic the phosphorylation event, increases the localization of VAChT to LDCVs. Conversely, the VMATs contain two glutamates upstream of their dileucine-like motif, and replacement of these residues by alanine conversely reduces sorting to LDCVs. The results provide some of the first information about sequences involved in sorting to LDCVs. Since the location of the transporters determines which vesicles store classical neurotransmitters, a change in VAChT trafficking due to phosphorylation may also influence the mode of transmitter release.

Key words: neurotransmitter • kinase • trafficking • exocytosis • monoamine

Introduction

At least two distinct populations of secretory vesicles mediate the regulated exocytotic release of neurotransmitters. Synaptic vesicles (SVs)[1] appear almost exclusively in nerve terminals where they cluster at the synaptic cleft (Calakos and Scheller, 1996). In contrast, large dense core vesicles (LDCVs) appear throughout the cell, and release transmitter more slowly and in response to different stimuli than SVs (De Camilli and Jahn, 1990; Martin, 1994). Although SVs are generally considered to contain classical transmitters, whereas LDCVs store neural peptides, both types of regulated secretory vesicles contain monoamines, indicating the potential for release of a single transmitter through two distinct mechanisms (Thureson-Klein, 1983; Bruns and Jahn, 1995). Since classical transmitters, including monoamines, are synthesized in the cytoplasm, the subcellular location of the transporters required for packaging them into secretory vesicles determines the site of vesicular storage, and hence, the mode of exocytotic release.

Secretory vesicles exhibit four distinct neurotransmitter transport activities, including one for monoamines, a second for acetylcholine (ACh), a third for γ-aminobutyric acid (GABA), and a fourth for glutamate (Liu and Edwards, 1997b). All of these activities depend on the H^+ electrochemical gradient across the vesicle membrane, and exchange lumenal protons for cytoplasmic transmitter (Schuldiner et al., 1995). Pharmacologic manipulation of vesicular transport indicates the importance of these activities for behavior. The antihypertensive drug reserpine inhibits vesicular monoamine transport and induces a syndrome resembling depression (Frize, 1954). In addition, amphetamines induce efflux from vesicular monoamine stores (Sulzer et al., 1995) and can cause psychosis. Thus,

Address correspondence to R.H. Edwards, UCSF School of Medicine, 513 Parnassus Avenue, San Francisco, CA 94143-0435. Tel.: (415) 502-5687. Fax: (415) 502-5687. E-mail: edwards@itsa.ucsf.edu

[1]*Abbreviations used in this paper:* ACh, acetylcholine; BIS, bisindolylmaleimide I; GABA, γ-aminobutyric acid; GST, glutathione S-transferase; HA, hemagglutinin; LDCVs, large dense core vesicles; PKC, protein kinase C; PNS, postnuclear supernatant; SGII, secretogranin II; SLMVs, synaptic-like microvesicles; SVs, synaptic vesicles; syn^+, synaptophysin positive; TMD, transmembrane domain; VAChT, vesicular acetylcholine transporter; VMATs, vesicular monoamine transporters.

changes in vesicular transport activity have the potential to influence behavior, but the extent to which they undergo regulation has remained unknown.

Molecular cloning has begun to identify the proteins responsible for neurotransmitter transport into secretory vesicles. One family of proteins includes two vesicular monoamine transporters (VMATs) and the vesicular acetylcholine transporter (VAChT). VMAT1 is expressed principally in peripheral, nonneural tissues and VMAT2 is expressed by central monoamine neurons (Varoqui and Erickson, 1997; Liu and Edwards, 1997b). Consistent with the observed release of monoamines from both SVs and LDCVs, the VMATs occur on multiple populations of secretory vesicles. In brain, VMAT2 localizes preferentially to LDCVs, but also resides on SVs, as well as tubulovesicular structures in the cell body and dendrites of central dopamine neurons (Nirenberg et al., 1995, 1996). Similarly, VMAT2 resides predominantly on LDCVs rather than the synaptic-like microvesicles (SLMVs) present in PC12 cells (Liu et al., 1994; Erickson et al., 1996). In contrast, VAChT localizes predominantly to SVs in brain (Gilmor et al., 1996; Weihe et al., 1996) and to lighter membranes, including the SLMVs in PC12 cells (Liu and Edwards, 1997a; Varoqui and Erickson, 1998). However, VAChT also occurs at lower levels on LDCVs in PC12 cells (Liu and Edwards, 1997a) and in neurons (Lundberg et al., 1981; Agoston and Whittaker, 1989). Thus, two closely related vesicular neurotransmitter transporters localize to distinct populations of secretory vesicles that differ in their mode of release.

To understand how VMAT2 and VAChT localize to different secretory vesicles, we have sought to identify their sorting signals. As integral membrane proteins, the transporters presumably depend on signals in their cytoplasmic domains that interact with a cytosolic sorting machinery. We have found previously that dileucine motifs located COOH-terminal to transmembrane domain (TMD) 12 of both VMAT2 and VAChT (see Fig. 1 A) mediate internalization of the transporters from the plasma membrane (Tan et al., 1998). Dileucine motifs implicated in the endocytosis of certain other proteins require the presence of acidic residues at positions −4 and −5 relative to the two leucines (Pond et al., 1995; Dietrich et al., 1997) and the VMATs contain highly conserved glutamates at both of these positions. However, replacement of these glutamates with alanine does not impair the internalization of VMAT2 (Tan et al., 1998). Since dileucine motifs mediate trafficking at multiple sites in the secretory pathway, these residues may influence other events, distinct from endocytosis. Although VAChT, like the VMATs, contains a glutamate at −4 relative to the dileucine, it contains a serine at −5, raising the possibility that the charge of this residue accounts for the localization of the transporters to distinct populations of secretory vesicles. In addition, the presence of a serine at −5 relative to the dileucine in VAChT suggests that phosphorylation of this residue may influence the sorting of the transporter. Indeed, phosphorylation of serine residues at −5 relative to the dileucine motifs in CD4 (Shin et al., 1991) and CD3γ (Dietrich et al., 1994) dramatically influences the trafficking of these proteins.

We now report that the serine at −5 relative to the dileucine motif in VAChT (Ser-480) undergoes phosphorylation by a calcium-dependent isoform of protein kinase C (PKC). Replacement of Ser-480 by alanine, which prevents phosphorylation, reduces the expression of VAChT on LDCVs relative to the wild-type protein. In contrast, substitution of Ser-480 by glutamate, to mimic the sequence of VMAT2 at this position and the phosphorylation event, increases the expression of VAChT on LDCVs. Consistent with the importance of acidic residues upstream of a dileucine motif in sorting to LDCVs, replacement of Glu-478 and -479 upstream of the dileucine-like motif in VMAT2 reduces localization to LDCVs. The results provide some of the first information about signals involved in sorting to different classes of secretory vesicles. In addition, they suggest that phosphorylation regulates the targeting of VAChT to LDCVs, providing a potential mechanism to regulate transmitter release.

Materials and Methods

Cell Culture

All cultures were grown in media containing penicillin and streptomycin at 37°C in 5% CO_2. Monkey kidney COS cells were maintained in DME containing 10% calf serum. PC12 cells were maintained in DME containing 5% calf serum and 10% equine serum (Greene and Tischler, 1976). For transient transfection, COS cells were electroporated with 15–20 μg DNA using a BioRad Gene Pulser (Peter et al., 1994). Stable PC12 cell transfectants expressing hemagglutinin (HA)-tagged transporters were prepared by electroporation of wild-type and mutant VAChT cDNAs in a modified pCDNA3 expression vector (see below). After selection in G418, isolated colonies (~80 per construct) were picked and screened for expression by immunofluorescence. At least two independently isolated cell lines were analyzed for each VAChT construct.

Mutagenesis and Subcloning

We used the method of Kunkel et al. (1991) to introduce epitope tags and point mutations into the VAChT cDNA. In brief, we prepared single-stranded uracil-containing template in the dut^-, ung^- CJ236 strain of *E. coli*, annealed the mutagenic primer, extended with T7 DNA polymerase, and transformed the reaction product into XL1-Blue. Oligonucleotides containing silent restriction enzyme sites to facilitate mapping were synthesized using an Applied Biosystems PCR-Mate. The mutations were verified by sequence analysis and a small fragment containing the desired mutation transferred into the wild-type VAChT cDNA in the expression vector pCDNA3 (Invitrogen) with an RSV promoter replacing the original CMV promoter. For expression of bacterial glutathione S-transferase (GST) fusion proteins (Smith and Johnson, 1988), cDNA fragments of wild-type and mutant VAChT were cut at VAChT nucleotide 1,473 using StuI and the multiple cloning site of the parent construct, and the 0.4-kb fragment inserted in frame into the SmaI site of the pGEX-5X-1 bacterial expression vector (Pharmacia Biotech).

Metabolic Labeling and Immunoprecipitation

For metabolic labeling with $^{32}P_i$, cells were washed three times in media lacking phosphate, and incubated for 4 h at 37°C in the presence of 0.5–1.0 mCi/ml $^{32}P_i$ (ICN). For kinase stimulation experiments, pharmacological agents at the concentrations indicated in the text were added from stock solutions by rapid mixing during the last 15 min of labeling. After labeling, the cells were washed in ice-cold PBS and harvested by scraping into 1 ml 50 mM Tris-HCl, pH 7.5, 150 mM NaCl, 50 mM NaF, 0.2 mM Na_3VO_4, 10 mM EDTA, 5 mM EGTA, 10 μg/ml PMSF, 2 μg/ml leupeptin, 2 μg/ml pepstatin, 1% vol/vol Triton X-100 detergent (homogenization buffer, HB). After removal of the nuclei and cell debris by centrifugation at 14,000 *g* for 5 min at 4°C, SDS was added to the supernatant to a final concentration of 0.2%. For immunoprecipitation, the mixture was incubated overnight at 4°C with either the polyclonal antiserum to VAChT prebound to protein A–Sepharose (Sigma Chemical Co.) or with an mAb to HA (Berkeley Antibody Co.) prebound to protein G–Sepharose. Immune complexes were washed 4 times in HB containing 0.2% SDS, resuspended

in 2× Laemmli sample buffer and the proteins separated by electrophoresis through 10% polyacrylamide. The gels were then fixed in 10% acetic acid, 50% methanol, dried, and submitted to autoradiography.

Western Analysis

Proteins were separated by electrophoresis through polyacrylamide containing SDS and transferred to nitrocellulose or PVDF using either a semidry or liquid transfer apparatus. The filters were then incubated in PBS containing 0.1% Tween 20 and 5% nonfat dry milk, and stained in the same buffer with either a primary rabbit polyclonal antibody to VAChT at 1:1,000 (Liu and Edwards, 1997a) or an mAb to HA (Berkeley Antibody Co.) at 1:1,000, followed by the appropriate secondary antibody conjugated to HRP (1:1,000). The complex was then visualized by chemiluminescence (Pierce Chemical Co.), and the exposed films scanned using a UMAX flatbed scanner and Adobe Photoshop for Macintosh. The digitized images were quantitated using NIH Image 1.61 software.

Phosphoamino Acid Analysis

Phosphoamino acid analysis was performed as previously described (Krantz et al., 1997). In brief, extracts prepared from cells metabolically labeled with $^{32}P_i$ were immunoprecipitated with the polyclonal antiserum to VAChT as described above, and the immunoprecipitates separated by electrophoresis through polyacrylamide. After autoradiography, the radiolabeled band was excised from the gel, rehydrated in 50 mM ammonium bicarbonate, and the protein was eluted overnight in 0.2% SDS, 2% β-mercaptoethanol. The eluate was precipitated with 20% TCA and partially hydrolyzed by boiling in 5.7 M HCl for 60 min. The hydrolysate was washed first with distilled water, then with 7.8% acetic acid, 2.2% formic acid (pH 1.9 buffer), resuspended in 10 μl pH 1.9 buffer containing phosphoamino acid standards, and spotted onto thin layer cellulose plates. Electrophoresis was performed at 4°C using pH 1.9 buffer for the first dimension and 5% acetic acid, 0.5% pyridine (pH 3.5 buffer) for the second dimension. The standards were then stained with ninhydrin and the plates submitted to autoradiography.

In Vitro Phosphorylation

To express GST fusion proteins, *Escherichia coli* were grown overnight in 1.6% tryptone, 1% yeast extract, 0.5% NaCl (2× YTA media) at 37°C, and induced in 0.1 mM isopropyl β-D-thiogalactoside (IPTG) for an additional 3–6 h at room temperature. Bacteria were then pelleted, resuspended in PBS, and disrupted by vigorous sonication for 1–2 min at 0°C. Cell debris was removed by centrifugation at 14,000 *g* and the resulting supernatant was either used immediately or stored at −70°C. To partially purify the fusion protein, the cleared extract was bound to glutathione-Sepharose beads for 20 min at room temperature in PBS, washed twice in PBS, and once in either 20 mM Tris, pH 7.5, 0.5 mM DTT, 10 mM $MgCl_2$ (lysate kinase buffer, LKB), or 50 mM MES, pH 6.0, 1.25 mM EGTA, 12.5 mM $MgCl_2$ (PKC buffer, PKCB). Aliquots of fusion protein (~1 μg) bound to glutathione-sepharose (10–20 μl bed vol) were then incubated with either 1 μl postnuclear supernatant (PNS; ~10 μg total protein) from COS or PC12 cells (see below) for 20 min at 30°C in LKB containing 2 mM $CaCl_2$, unless otherwise indicated, and 200 μM ATP and γ[^{32}P]ATP, to a final specific activity of 500 μCi/μmol; or with 20 ng (0.02 units) of the catalytic fragment of PKC from rat brain (PKC-M; Calbiochem) for 20 min at 30°C in PKCB containing 125 μM ATP and γ[^{32}P]ATP, to a final specific activity of 5,000 μCi/μmol. For experiments using kinase inhibitors, the ATP concentration was reduced to 1 μM. The reactions were stopped by washing with cold PBS containing 15 mM EDTA, the phosphorylated proteins were eluted with 20 μl of 10 mM glutathione in 50 mM Tris-HCl, pH 8.0, and the eluates were added to an equal volume of 2× Laemmli sample buffer before separation by electrophoresis through 12.5% polyacrylamide. The gels were fixed and stained with Coomassie blue, and then dried and submitted to autoradiography.

Preparation of a PNS was performed as previously described (Krantz et al., 1997). In brief, cells were harvested using either trypsin or a cell scraper after one freeze–thaw cycle. The cells were resuspended in 10 mM Hepes-KOH, pH 7.4, 320 mM sucrose, 10 mM EDTA, 5 mM EGTA, 20 μg/ml PMSF, 2 μg/ml leupeptin, 2 μg/ml pepstatin, 1 mM DTT (resuspension buffer), and disrupted in a bath sonicator (Branson) using 15 pulses at an intermediate setting. Nuclei and cell debris were removed by sedimentation at 1,300 *g* for 5 min at 4°C, and the supernatant stored at −70°C before use. To reduce competition with kinase inhibitors, the endogenous ATP in the added cell extract was reduced tenfold by dilution in resuspension buffer, followed by reconcentration to the original volume by filtration through a Centricon 10 filtration device (Amicon).

Immunofluorescence

For immunostaining, PC12 cells were plated onto glass coverslips coated with poly-D-lysine and Matrigel (Collaborative Research), and treated with 50 ng/ml NGF for 2–5 d before fixation in 100 mM $NaPO_4$, pH 7.3 containing 4% paraformaldehyde. The cells were then permeabilized in PBS, pH 7.4, containing 5% bovine serum and 0.1% TX-100 detergent, incubated with primary antibody in the same buffer (1:100–1:1,000), washed three times for 5 min, and incubated in secondary antibody (1:100) for 1 h. After washing, the coverslips were mounted onto glass slides using Antifade (Molecular Probes), and visualized by indirect immunofluorescence with a BioRad 1024 confocal microscope. Digital images were processed using NIH Image and Adobe Photoshop.

Sucrose Gradient Equilibrium Centrifugation

To label the dense core granules with [^{3}H]serotonin, PC12 cells were incubated in standard medium containing 5 μCi [^{3}H]serotonin (Amersham)/15 ml for at least 4 h before cell fractionation. Cell membranes were prepared by homogenization at a clearance of 10 μm in cold Hepes-KOH-buffered saline (HBS) containing 2 mM Mg EGTA, 1 μg/ml leupeptin, 1 μg/ml pepstatin, and 10 μg/ml PMSF. The nuclei and other cell debris were pelleted by centrifugation at 1,300 *g* for 5 min. For sucrose gradient equilibrium centrifugation, the PNS was layered onto a linear 0.65–1.55 M (or 0.6–1.6 M, as indicated) sucrose gradient in 10 mM Hepes-KOH and sedimented to equilibrium at 30,000 rpm for 8–12 h in an SW41 rotor at 4°C. 17 fractions were collected from the bottom of the tube, stored at −70°C, and the radioactivity of fractions from cells preloaded with [^{3}H] serotonin measured in Ecolume (ICN) using a Beckman 3800 scintillation counter. For two-step separations, the PNS from cell lysates was first layered onto a linear 0.3–1.2 M sucrose velocity gradient in 10 mM Hepes and sedimented at 25,400 rpm for 30 min in an SW41 rotor at 4°C. The radioactivity in each fraction of the velocity gradient was determined by scintillation counting, the two peak fractions were pooled, adjusted to a final sucrose concentration of 0.6 M, layered onto a linear 0.6–1.6 M sucrose gradient, and sedimented to equilibrium at 30,000 rpm for 8–12 h in an SW41 rotor at 4°C, with 12 fractions collected from the bottom of the tube. Immunoblots were probed using an antibody to the HA epitope tag, and were then optically scanned and the digitized images quantitated using NIH Image software. The total amount of HA immunoreactivity in each fraction of the second gradient was expressed as a percentage of the total HA immunoreactivity in the PNS loaded onto the first gradient, or

$$\frac{\text{HA immunoreactivity in each fraction}}{\text{HA immunoreactivity in PNS}} \times 100,$$

as shown in Fig. 9 as

$$\frac{\text{HA immunoreactivity fraction (\%)}}{\text{PNS}}.$$

Using secretogranin II (SgII) and ^{3}H-serotonin as markers, fractions 7–10 of the second gradient include the peak of LDCVs. The sum of HA immunoreactivity for fractions 7–10 of the second gradient was then normalized for the recovery of LDCVs as follows:

$$\frac{\text{HA immunoreactivity fraction (\%)}}{\text{PNS}} \times \frac{\dfrac{[^3\text{H}]\text{serotonin in fraction 7–10 of index gradient}}{[^3\text{H}]\text{-serotonin in index PNS}}}{\dfrac{[^3\text{H}]\text{serotonin in fraction 7–10 of wild-type gradient}}{[^3\text{H}]\text{serotonin in wild-type PNS}}}.$$

This measure is similar to a recently described granule targeting index (Blagoveshchenskaya et al., 1999). Note that the number of fractions collected from one-step and two-step procedures were not identical, and that LDCVs therefore localize to different fractions.

Immunoisolation

Magnetic beads conjugated to secondary mouse antibody (Dynal) were

coated with antisynaptophysin mouse mAb by incubation overnight in PBS, pH 7.4, containing 2% FCS (immunoisolation buffer), followed by 4 washes in this buffer. For each reaction, 10 μl bead slurry was added to 30 μl PNS and mixed for 1 h at 4°C. After washing in immunoisolation buffer, the bound material was eluted in 2× Laemmli sample buffer, subjected to Western analysis in parallel with samples of starting material diluted to yield images of comparable intensity, and quantitated using Adobe Photoshop and NIH image. We then expressed the amount of VAChT in the immunoisolated material as a fraction of the amount of VAChT in the starting material.

Immunoelectron Microscopy

Undifferentiated PC12 cells were fixed for 2 h at room temperature with a mixture of 2% formaldehyde and 0.2% glutaraldehyde in 0.1 M phosphate buffer, pH 7.4, and stored in 4% formaldehyde until further processing. Ultrathin cryosectioning was performed according to the method described by Liou et al. (1996) and double immunogold labeling as described by Slot et al. (1991). Labeling was carried out with the polyclonal antibody to VAChT, which labeled only PC12 cells overexpressing wild-type or mutant VAChT. For double-labeling with synaptophysin, we used a polyclonal rabbit antiserum (Synaptic Systems). Semiquantitative analysis of the relative subcellular distributions of the S480A and S480E mutants was performed in double-blind experiments. To establish the percentage of total label that was present on LDCVs, sections were scanned along a fixed track and the gold particles associated with LDCVs determined as a proportion of all gold particles no more than 25 nm from a membrane. In a separate measurement, we used a similar approach to determine the association of gold particles with LDCVs relative to the association with ~50-nm vesicles. The latter category includes SLMVs, but may also include Golgi-derived vesicles and constitutively recycling vesicles of a similar size. For all quantitations, 1,000 gold particles were counted in ten separate counting sessions using at least two independently labeled grids.

Results

We first used heterologous expression in COS cells to determine whether VAChT undergoes regulation by phosphorylation. Like the VMATs, VAChT sorts to endocytic vesicles in these cells (Liu et al., 1994; Liu and Edwards, 1997a) and the acidic nature of this compartment supports the transport activity observed in biochemical studies (Liu et al., 1992). To facilitate the analysis, we previously engineered an epitope from HA into the lumenal loop between TMDs 1 and 2 of VAChT, as well as VMAT2. These epitope tags do not interfere with the transport activity or subcellular localization of either transporter (Tan et al., 1998).

Phosphorylation of VAChT on Ser-480

To assess the phosphorylation of VAChT, we used metabolic labeling with $^{32}P_i$. Immunoprecipitation with an HA antibody of COS cells labeled continuously with $^{32}P_i$ for 4 h shows a prominent labeled protein of ~70 kD in cells transiently transfected with the VAChT cDNA (Fig. 1 B, right). The strongly labeled protein corresponds to the largest immunoreactive species of VAChT observed in transfected cells by Western analysis with an antibody to VAChT (Fig. 1 B, left). An ~50-kD immature form of VAChT (Liu and Edwards, 1997a) and an ~35-kD immunoreactive species undergo phosphorylation to a lesser extent (Fig. 1, B and D). The amount of protease inhibitors used to prepare the cell extracts influences the amount of the ~35-kD form, suggesting that it results from proteolytic degradation (data not shown), but we have used the optimal cocktail of protease inhibitors for these experiments, and not observed substantial variation in the recovery of full length VAChT. Recognition by the COOH-terminal antibody to VAChT, but not the more NH_2-terminal antibody to the HA tag suggests that the ~35-kD species represents a phosphorylated COOH-terminal fragment (compare Figs. 1 B and 2 A). The analysis of VMAT2–VAChT chimeras further supports localization of a phosphorylation site(s) to the COOH terminus (data

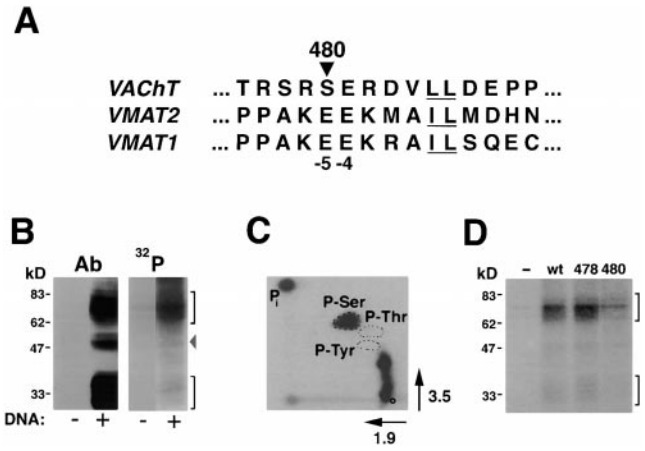

Figure 1. Phosphorylation of VAChT on Ser-480 in COS cells. A, Alignment of the sequences surrounding the dileucine motifs (underlined) in the COOH termini of VMAT1, VMAT2, and VAChT. All three transporters show a glutamate at position −4 relative to the dileucine motif. The VMATs also contain a glutamate at the −5 position. In contrast, VAChT contains a serine at the equivalent position, serine 480 (Ser-480), surrounded by several arginines that form a consensus sequence for phosphorylation by PKC and other basic residue-directed kinases (Pearson and Kemp, 1991). B, Phosphorylation of VAChT in COS cells. Using COS cells transiently transfected with the cDNA encoding VAChT (+) or no DNA (−), the left shows Western analysis with a rabbit antibody to VAChT. In the right, cells metabolically labeled with $^{32}P_i$ were immunoprecipitated with the same VAChT antiserum. Of the ~70-kD (black bracket), ~50-kD (arrowhead), and ~35-kD immunoreactive species (gray bracket), VAChT undergoes phosphorylation predominantly on the ~70-kD form. The ~50-kD species and the ~35-kD doublet appear to undergo less prominent labeling. In the case of the ~35-kD species, the reduced labeling results at least partly from the inefficiency of immunoprecipitation (data not shown). C, Phosphoamino acid analysis of VAChT. Immunoprecipitated VAChT was excised from the gel, hydrolyzed in hydrochloric acid, and the hydrolysate separated by thin-layer electrophoresis, using pH 1.9 for the first dimension and pH 3.5 for the second dimension. Autoradiography shows radiolabeled material comigrating with the phosphoserine (P-Ser) standard, but not with the phosphothreonine (P-Thr) or phosphotyrosine (P-Tyr) standards. Phosphopeptides resulting from incomplete hydrolysis migrate as a smear in the second dimension. Free $^{32}P_i$ migrates at the position shown (P_i), and the origin is circled. D, VAChT undergoes phosphorylation on Ser-480. COS cells transiently transfected with cDNAs encoding wild-type VAChT (wt), with mutant cDNAs containing alanine replacements at Ser-478, Ser-480, or with no DNA (−) were metabolically labeled with $^{32}P_i$, immunoprecipitated with the VAChT antibody, and subjected to SDS-PAGE, followed by autoradiography. Mutation of Ser-480, but not Ser-478, reduced phosphorylation of the mature form of VAChT (black bracket) and the COOH-terminal fragment (gray bracket). Molecular weight markers (kD) are shown to the left in B and D.

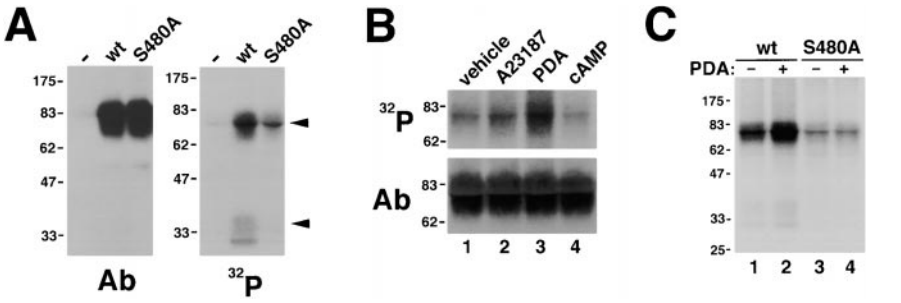

Figure 2. Phosphorylation of VAChT by PKC in PC12 cells. A, Untransfected PC12 cells (−), cells stably expressing HA-tagged wild-type VAChT (wt), and cells expressing mutant VAChT with an alanine replacement at Ser-480 (S480A) were metabolically labeled with $^{32}P_i$, immunoprecipitated with an antiserum against VAChT, and subjected to SDS-PAGE, followed by autoradiography (right), or blotted to nitrocellulose and immunostained with an mAb to the HA tag (left). The mature ~70-kD and the ~35-kD doublet forms of VAChT undergo phosphorylation (see arrowheads). Substitution of Ser-480 by alanine reduces phosphorylation of the ~70-kD form and eliminates phosphorylation of the ~35-kD doublet without affecting the levels of the mature VAChT protein (left). Note that the mAb to HA does not recognize the ~35-kD doublet as seen in the immunoblot, presumably because these species are COOH-terminal fragments that do not contain the more NH_2-terminal HA tag. B, Regulation of VAChT phosphorylation. PC12 cells stably expressing wild-type HA-tagged VAChT were metabolically labeled for 4 h with $^{32}P_i$, treated for 15 min with vehicle alone (DMSO; lane 1), 10 μM A23187 (lane 2), 3 μM phorbol diacetate (PDA; lane 3), or 1 mM 8-bromo-cyclic AMP (cAMP) with 1 mM of the phosphodiesterase inhibitor 3-isobutyl-1-methylxanthine (lane 4), and the extracts either immunoprecipitated for VAChT (top), or transferred to nitrocellulose and immunostained for HA (bottom). VAChT shows a robust increase in phosphorylation with PDA, and a smaller increase in phosphorylation with A23187. A small decrease in phosphorylation occurs with increased cAMP (lane 4). C, Regulation of Ser-480 phosphorylation. PC12 cells stably expressing wild-type HA-tagged VAChT (lanes 1 and 2) and cells expressing mutant VAChT with an alanine replacement at Ser-480 (S480A; lanes 3 and 4) were metabolically labeled with $^{32}P_i$, treated for 15 min with vehicle alone (−; lanes 1 and 3) or 3 μM phorbol diacetate (PDA; lanes 2 and 4) and immunoprecipitated as in B. Replacement of Ser-480 with alanine greatly reduces PDA-induced phosphorylation of VAChT.

not shown). Since the COOH terminus of VAChT contains serine, threonine, and tyrosine residues that might serve as phosphorylation sites, we performed phosphoamino acid analysis of the VAChT protein expressed in COS cells and metabolically labeled with $^{32}P_i$ (Boyle et al., 1991). Hydrolysates of immunoprecipitated VAChT contain phosphoserine, but not phosphothreonine or phosphotyrosine residues, indicating that phosphorylation of VAChT occurs exclusively on serine (Fig. 1 C).

Although the COOH terminus of VAChT contains several serine residues, we have focused on Ser-478 and -480 (Fig. 1 A). Both of these residues show strong conservation in vertebrates (Erickson et al., 1994; Roghani et al., 1994; Naciff et al., 1997) and reside within a consensus sequence for phosphorylation by multiple kinases including PKC (Pearson and Kemp, 1991). In addition, Ser-480 occurs five residues upstream from the dileucine motif required for efficient internalization of VAChT from the plasma membrane (Tan et al., 1998) and the VMATs contain a highly conserved glutamate at the equivalent position (Liu et al., 1992; Erickson and Eiden, 1993; Krejci et al., 1993). Further, an acidic residue at the −5 position relative to a dileucine motif influences the sorting of other membrane proteins (Pond et al., 1995) and phosphorylation at this position regulates the trafficking of CD3γ and CD4 (Shin et al., 1991; Dietrich et al., 1994). To determine whether VAChT undergoes phosphorylation on Ser-480 or Ser-478, we used site-directed mutagenesis (Kunkel et al., 1991) to replace these residues individually with alanine. Metabolic labeling and immunoprecipitation of the mutants expressed in COS cells shows reduced phosphorylation of the S480A, but not the S478A mutant (Fig. 1 D). Although the S480A mutant shows low levels of residual phosphorylation on the ~70-kD species, the mutation eliminates labeling of the COOH-terminal ~35-kD fragment (Fig. 1 D, also see 2 A). Simultaneous mutagenesis of both Ser-478 and Ser-480 did not further reduce the phosphorylation (data not shown). Thus, the COOH terminus of VAChT appears to undergo phosphorylation predominantly, if not solely, on Ser-480.

To extend the analysis of VAChT phosphorylation to neuroendocrine cells, we used heterologous expression in rat pheochromocytoma PC12 cells. Metabolic labeling with $^{32}P_i$ of PC12 transformants stably expressing VAChT shows prominent labeling of an ~70-kD band not observed in untransfected cells (Fig. 2 A, right). As in COS cells, the S480A mutation greatly reduces the labeling of both this band and the ~35-kD species, and Western analysis of the cell extracts confirms the equivalent expression of both wild-type and mutant VAChT (Fig. 2 A, left). Thus, phosphorylation of the VAChT COOH terminus occurs on Ser-480 in both COS and PC12 cells.

Regulation by PKC

To determine whether VAChT phosphorylation undergoes regulation, we have pharmacologically stimulated several protein kinases in the stably transfected PC12 cells. Using the calcium ionophore A23187 in the presence of external calcium to activate such calcium-dependent kinases as CaMKII and facilitate phosphorylation by calcium-dependent (conventional) isoforms of PKC (cPKC), we found an increase in phosphorylation of VAChT (Fig. 2 B, lane 2) relative to untreated cells (Fig. 2 B, lane 1). Stimulation of cPKC and other PKC isoforms with the phorbol ester phorbol 12,13-diacetate (PDA) activates VAChT phosphorylation even more strongly (Fig. 2 B, lane 3). In contrast, stimulation of cAMP-dependent protein kinase (PKA) with the cell-permeable cAMP analogue 8-bromo-adenosine 3′,5′-cyclic monophosphate (8-Br-cAMP) modestly inhibits VAChT phosphorylation. These results suggest phosphorylation of VAChT by PKC,

with the potential for modulation by other signaling pathways. Mutagenesis of Ser-480 dramatically reduces PDA-induced changes in VAChT phosphorylation (Fig. 2 C), indicating that Ser-480 undergoes PKC-dependent phosphorylation.

To identify the kinase(s) responsible for phosphorylating VAChT, we have extended the analysis in vitro. As a substrate for phosphorylation, we produced a bacterial protein containing GST fused to the COOH terminus of VAChT (GST-VAChT). Since phosphorylation in vitro may show less specificity than in intact cells, we first tested the specificity of GST-VAChT phosphorylation. In the presence of $\gamma[^{32}P]$ATP and COS or PC12 cell lysate, GST-VAChT undergoes robust phosphorylation (Fig. 3, A and E). The replacement of Ser-480, but not Ser-478 with alanine abolishes this modification, consistent with the results of metabolic labeling in intact cells and indicating the specificity of in vitro phosphorylation for the appropriate residues (Fig. 3, A and E). Similar to the changes observed in cells with the calcium ionophore A23187, addition of Ca^{2+} to the in vitro reaction increases phosphorylation of the fusion protein (Fig. 3, B and E). Calmodulin does not further alter the response to increased Ca^{2+}, consistent with data from intact cells implicating Ca^{2+}-dependent isoforms of PKC, which do not require calmodulin for activation.

We used the in vitro phosphorylation reaction and specific inhibitors to identify the kinase(s) responsible for phosphorylating VAChT. The PKC inhibitor H7 partially blocks VAChT phosphorylation by COS (Fig. 3, C and D) or PC12 (Fig. 3 E) cell extracts, but H7 also inhibits such other kinases as PKA (Hidaka et al., 1984). We tested the effect of bisindolylmaleimide I (BIS), a highly specific PKC inhibitor (K_i ~0.01 μM) that inhibits other kinases only at much higher concentrations (K_i for PKA ~2 μM; Toullec et al., 1991). BIS inhibits phosphorylation of VAChT by ~50% at 0.1 μM, implicating PKC in VAChT phosphorylation. Increasing concentrations of BIS do not further reduce phosphorylation, suggesting that distinct kinase(s) may also contribute to VAChT phosphorylation. However, both peptide and nonpeptide inhibitors of PKA (H89; Chijiwa et al., 1990) and CamKII (KN93; Sumi et al., 1991) do not inhibit VAChT phosphorylation at concentrations that selectively inhibit these enzymes (data not shown). Thus, although the identity of the additional ki-

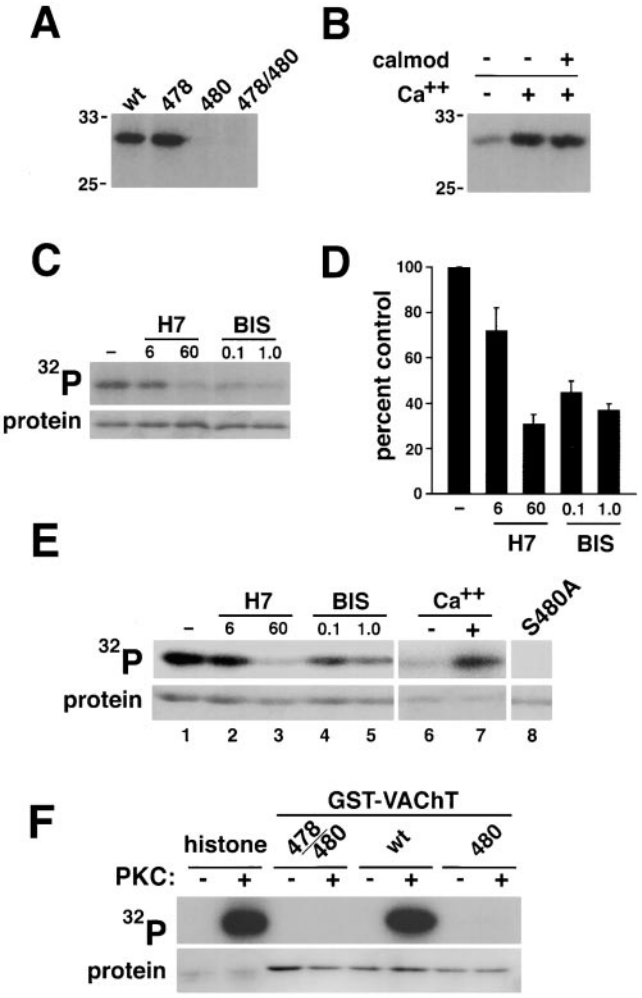

C, PKC inhibitors reduce VAChT phosphorylation. Wild-type VAChT fusion proteins were incubated as in A, but with the concentration of ATP lowered to 1 μM to reduce competition with kinase inhibitors. The PKC-selective inhibitor H7 (final concentration 6 or 60 μM), and the more PKC-specific BIS (final concentration 0.1 or 1 μM) or vehicle (−) were added before the lysate and $\gamma[^{32}P]$ATP. Coomassie blue staining confirmed the presence of similar amounts of fusion protein in each lane (bottom). D, Quantitative analysis of PKC inhibition. Autoradiographs of the kind shown in D were optically scanned, the digital images quantitated, and the values expressed as a percentage of samples treatment with vehicle alone (percent control). The average ± standard error of two independent experiments are shown. E, Phosphorylation of VAChT bacterial fusion proteins using PC12 cell lysate. Fusion proteins containing the COOH terminus of wild-type VAChT (lanes 1–7) or the VAChT mutant with an alanine replacement at Ser-480 (lane 8) were incubated with $\gamma[^{32}P]$ATP and a postnuclear PC12 cell supernatant for 20 min at 30°C with or without addition of the PKC inhibitors H7 or BIS, as described in C (lanes 1–5), or 2 mM calcium chloride (lanes 6 and 7). Coomassie blue staining confirmed the presence of similar amounts of fusion protein (bottom). F, Phosphorylation of VAChT bacterial fusion proteins by purified PKC. Fusion proteins containing wild-type VAChT (wt) or VAChT mutants with alanine replacements at Ser-480 or both Ser-478 and Ser-480 (478/480), or histone H1 as a positive control were incubated with $\gamma[^{32}P]$ATP and the catalytic fragment of PKC for 20 min at 30°C. Similar to histone H1, the fusion protein containing wild-type VAChT shows robust phosphorylation. Mutation of Ser-480, or both Ser-478 and Ser-480, eliminates phosphorylation by PKC.

Figure 3. In vitro phosphorylation of VAChT on Ser-480. A, Phosphorylation of wild-type and mutant VAChT bacterial fusion proteins. Fusion proteins containing GST joined in frame to the COOH terminus of wild-type VAChT (wt) or VAChT mutants with alanine replacements at Ser-478, Ser-480, or both Ser-478 and Ser-480 (478/480) were incubated with $\gamma[^{32}P]$ATP and a postnuclear COS cell supernatant for 20 min at 30°C. The proteins were then separated by electrophoresis and submitted to autoradiography. The fusion protein containing wild-type VAChT showed robust phosphorylation. Mutation of Ser-480 or both Ser-478/480, but not Ser-478 alone eliminates phosphorylation. Staining with Coomassie blue showed similar levels of fusion protein in each lane (data not shown). B, Calcium increases VAChT phosphorylation. Wild-type VAChT fusion proteins were incubated as in A with and without 2 mM calcium chloride, and 2.4 μM calmodulin. The addition of calcium potentiates VAChT phosphorylation, implicating a calcium-activated kinase.

nases remains unclear, the effects of calcium, PDA, and BIS on VAChT phosphorylation suggest that a calcium- and diacylglycerol-activated form of PKC mediates phosphorylation of the transporter at Ser-480. Indeed, purified PKC robustly phosphorylates Ser-480 in vitro (Fig. 3 F). These results are consistent with a previous report showing that VAChT undergoes PKC-dependent phosphorylation in synaptosomes prepared from hippocampus (Barbosa et al., 1997).

Ser-480 and VAChT Localization

Previous structural analysis of the VMATs and VAChT has implicated the central region containing 12 TMDs in the translocation of substrate (Merickel et al., 1995; Finn and Edwards, 1998). In contrast, the COOH termini appear to be required for localization rather than transport (Tan et al., 1998). Nonetheless, we compared the ACh transport activity of PC12 cells expressing the wild-type protein with that of cells expressing the S480A mutant and a mutant in which Ser-480 was replaced by glutamate to mimic the phosphorylation event (S480E). Using a standard transport assay, the activities of the S480A and S480E mutants were similar to wild-type (data not shown), suggesting that phosphorylation of Ser-480 does not affect catalytic function.

Since COOH-terminal signals appear to govern the membrane trafficking of VMATs and VAChT (Tan et al., 1998; Varoqui and Erickson, 1998), we have focused on the possible role of phosphorylation at Ser-480 on the localization of VAChT using transfected PC12 cells stably expressing wild-type and mutant proteins. After treatment with nerve growth factor to induce neurite formation, double-staining shows extensive colocalization of wild-type VAChT with the endosome/SLMV marker synaptophysin in both the cell body and at the tips of processes (Liu and Edwards, 1997a; Fig. 4). To determine the role of phosphorylation in the localization of the wild-type protein, we used PDA to stimulate PKC, and tautomycin (100 nM) to inhibit protein phosphatases 1 and 2A, and observed a decrease in the perinuclear localization of wild-type VAChT (data not shown). However, the S480A mutant showed similar changes in localization after treatment with PDA and tautomycin, excluding a role for phosphorylation at this site in

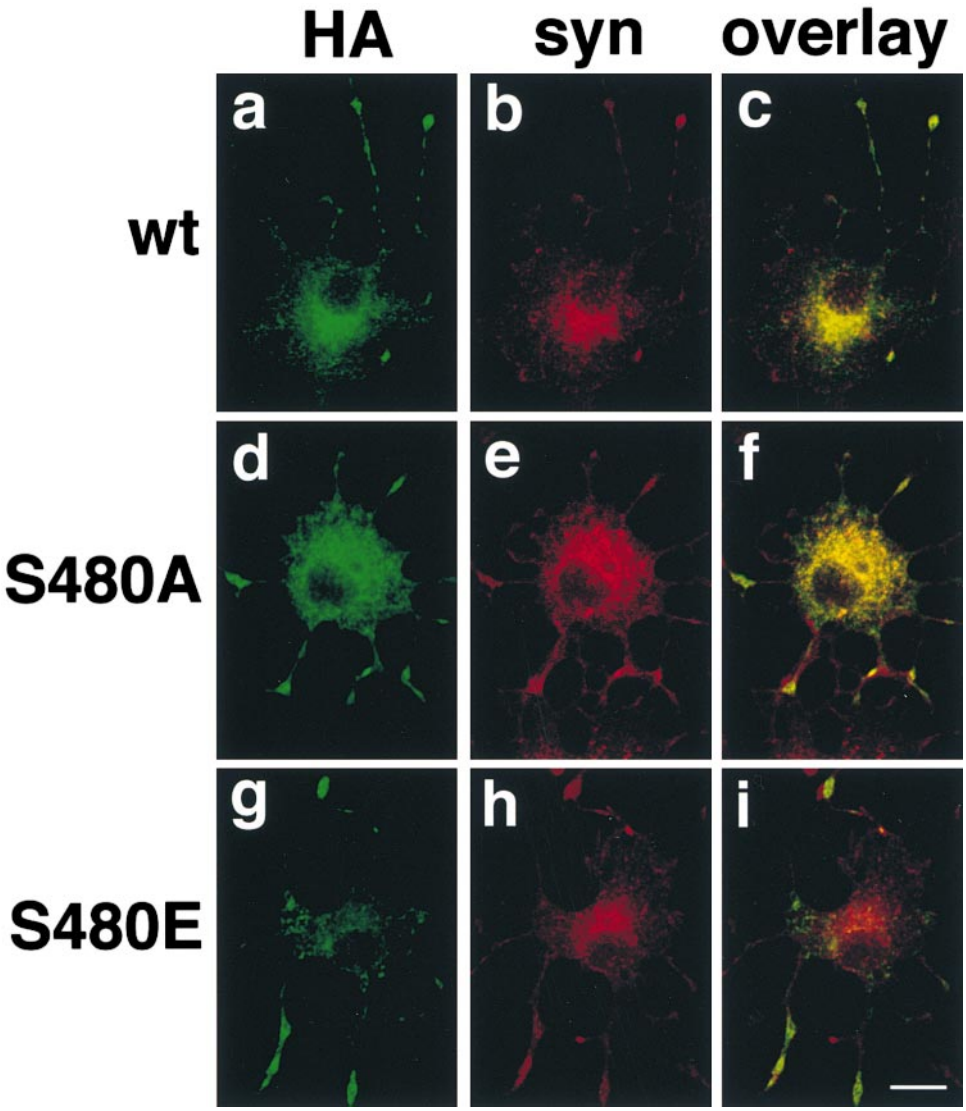

Figure 4. Mutation of Ser-480 influences localization of VAChT to endosomes and SLMVs. PC12 cells stably expressing HA-tagged wild-type VAChT, the S480A and S480E mutants were double-stained with a mouse mAb to HA (a, d, and g), and a rabbit polyclonal antibody to synaptophysin (syn; b, e, and h), a marker for endosomes and synaptic-like microvesicles (SLMVs). Visualized with the appropriate secondary anti-mouse antibodies conjugated to FITC (a, d, and g) and anti-rabbit antibodies conjugated to Texas red (b, e, and h), the cells were examined by confocal laser microscopy. The overlays of FITC and Texas red channels are shown in c, f, and i. Wild-type VAChT (a–c) and the S480A mutant (d–f) extensively, but incompletely colocalize with synaptophysin in cell bodies and processes. In contrast, the S480E mutant (g–i) resides primarily in processes. Bar, 10 μm.

the observed changes. Indeed, PKC and protein phosphatases contribute to many membrane trafficking events (Davidson et al., 1992; De Mattheis et al., 1993). To assess the specific role of Ser-480 phosphorylation on VAChT localization, we therefore used mutants that prevent (S480A) or mimic (S480E) phosphorylation specifically at this site.

The S480A mutant shows similar, extensive colocalization with synaptophysin, similar to wild-type VAChT. However, S480E localizes less with synaptophysin in the cell body. Rather, the distribution of S480E more closely resembles that of the LDCV marker SgII than wild-type VAChT or S480A (Fig. 5). The results suggest that an acidic residue −5 relative to the dileucine motif influences the steady-state distribution of VAChT.

To characterize further the effect of Ser-480 mutations on the membrane trafficking of VAChT, we have used density gradient fractionation (Liu et al., 1994). As noted previously, wild-type VAChT partially colocalizes with the SLMV/endosome marker synaptophysin in light fractions on equilibrium sedimentation gradients. However, VAChT localizes to additional compartments including LDCVs, and appears as a relatively broad peak extending into heavier fractions (Liu and Edwards, 1997a; Varoqui and Erickson, 1998). HA-tagged VAChT shows a similar distribution (Fig. 6 A). The S480A mutant also appears preferentially in light fractions (Fig. 6 B), and exhibits a single peak that coincides more precisely with the peak of synaptophysin than does wild-type VAChT. The S480E mutant, which mimics phosphorylation at Ser-480, also comigrates with synatophysin. However, S480E shows increased cofractionation with heavier membranes relative to wild-type VAChT and the S480A mutant (Fig. 6, C and D), confirming that an acidic residue at position −5 relative to the dileucine motif influences subcellular localization.

The immunofluorescence and fractionation experiments suggest that the Ser-480 mutations also change the expression of VAChT on SLMVs and/or endosomes. To further quantitate these differences, we immunoisolated vesicles expressing synaptophysin from cells expressing wild-type and mutant VAChT, and determined the amount of immunoreactive VAChT in synaptophysin-positive (syn^+) vesicles relative to the total amount in cell lysates (Fig. 6 E). The S480A mutant sorts to syn^+ vesicles in proportions similar to wild-type VAChT (~15%). The low proportion presumably reflects the localization of VAChT to multiple membrane compartments, suggested by the distribution on sucrose gradients, as well as, perhaps, the inefficiency of immunoisolation. In contrast to the wild-type protein and S480A, the S480E mutant localizes to syn^+ vesicles in lower proportions (~7%). Since synaptophysin resides on both endosomes and SLMVs in PC12 cells, the results indicate reduced expression of S480E on one or both of these membranes. To determine whether the Ser-480 mutations specifically affect sorting to SLMVs, we separated endosomes from SLMVs using velocity gradient sedimentation. However, we did not detect consistent differences in the proportion of wild-type and mutant VAChT expressed on SLMVs (data not shown), suggesting that the increase in targeting of S480E to heavy fractions on sucrose density gradients correlates primarily with a decrease in localization to syn^+ endosomes.

Altered Localization of a VMAT2 Mutant

Unlike VAChT, wild-type VMAT2 contains acidic residues at both positions −4 and −5 relative to the dileucine-like motif (Glu-478 and Glu-479; see Fig. 1). The importance of acidic charge upstream of the dileucine motif in

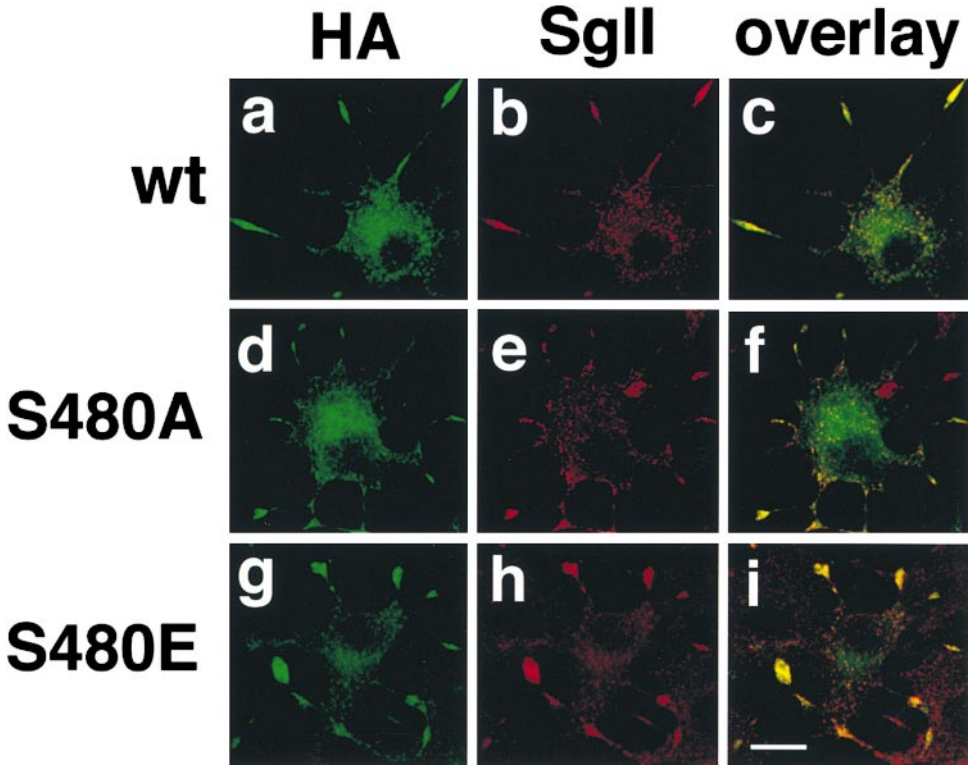

Figure 5. Mutation of Ser-480 alters the localization of VAChT to process tips. PC12 cells stably expressing wild-type VAChT, S480A, and S480E mutants were double-stained with a mouse mAb to the epitope tag (HA; a, d, and g), and a rabbit polyclonal antiserum to SgII (b, e, and h), a marker for LDCVs. Visualized with the appropriate secondary anti-mouse antibodies conjugated to FITC (a, d, and g) and anti-rabbit antibodies conjugated to Texas red (b, e, and h), the cells were examined by confocal microscopy. The overlays of FITC and Texas red channels are shown in c, f, and i. Wild-type VAChT (a–c) and S480A (d–f) partially colocalize with SgII at the tips of processes, but also occur at high levels in cell bodies. In contrast, S480E (g–i) colocalizes extensively with SgII in the tips of processes, and like SgII, shows less expression in cell bodies. Bar, 10 μm.

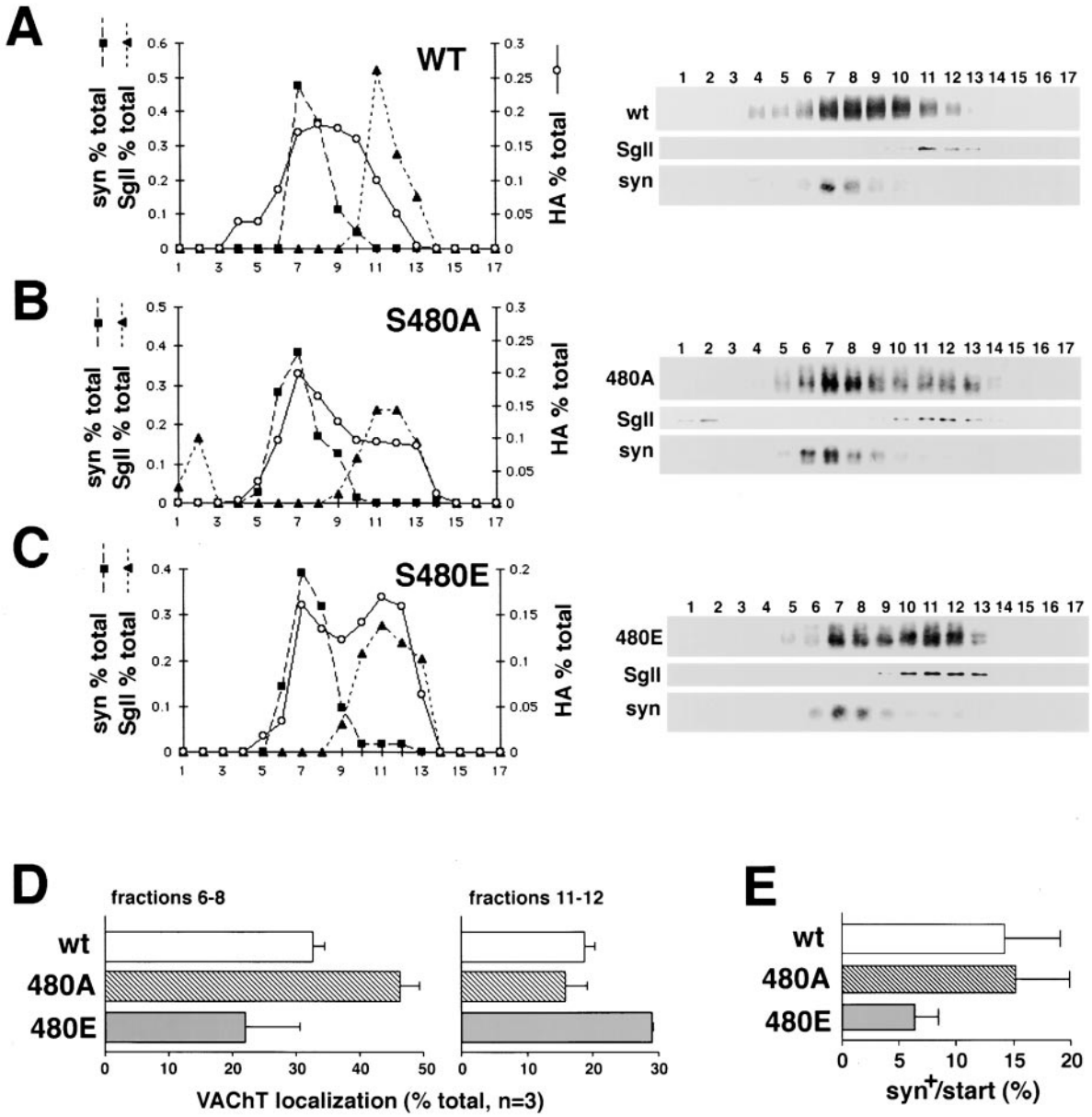

Figure 6. Density gradient fractionation of wild-type and mutant VAChT. PNSs of PC12 cells stably expressing HA-tagged wild-type VAChT (A), and mutants S480A (B) and S480E (C), were separated by equilibrium gradient centrifugation through 0.65–1.55 M sucrose. The fractions were submitted to Western analysis with the mAb to HA for VAChT (top of immunoblots in A, B, and C), a polyclonal antibody to the LDCV marker SgII (middle), and an mAb to the endosome/SLMV marker synaptophysin (syn; bottom). The gradients shown in A–C were digitized and quantified. For each fraction, the amount of HA-tagged VAChT, synaptophysin, and SgII was expressed as a percentage of the total immunoreactivity shown to the left of the immunoblots. Consistent with previous results (Liu and Edwards, 1997a), wild-type VAChT partially cofractionates with synaptophysin as a broad peak that also overlaps with fractions containing SgII. In contrast, S480A cofractionates well with synaptophysin. The mutant S480E mutant, on the other hand, fractionates with synaptophysin, but also shows a second peak that cofractionates with SgII in heavy fractions. D, The ratio of HA-tagged VAChT localized to light fractions 6–8 (left) or heavy fractions 11 and 12 (right) were expressed as a percentage of total HA immunoreactivity. The mean ± standard error ($n = 3$) were derived from the data shown in A–C, together with additional experiments using two independently derived cell lines for each mutant. E, Immunoisolation of synaptophysin-containing vesicles. PNSs from cell lines expressing wild-type VAChT, and the S480A and S480E mutants, were incubated with magnetic beads conjugated with an mAb to synaptophysin. Western blots of immunoisolated synaptophysin positive (syn^+) vesicles and starting lysate (start) were then immunostained using a polyclonal antiserum to VAChT. The amount of immunoisolated VAChT relative to the starting material was determined from digitized images and expressed as syn^+/start. The average ± SEM were determined from two independent experiments. Similar proportions of wild-type of S480A localize to syn^+ membranes, whereas the S480E mutant localizes approximately half as well, indicating the importance of a neutral residue at Ser-480 for sorting to light vesicles.

VAChT suggests that Glu-478 and Glu-479 may also affect VMAT2 trafficking. We therefore replaced Glu-478 and -479 with alanine (E478A/E479A). Immunofluorescence of stably transfected PC12 cells shows that wild-type VMAT2 colocalizes with the LDCV marker SGII at the tips of processes (Fig. 7, a–c). However, the E478A/E479A mutant differs from SGII and shows consistently strong labeling in cell bodies (Fig. 7, d–f). Indeed, the E478A/E479A mutant colocalizes with synaptophysin to a greater extent than wild-type VMAT2 (Fig. 7, g–l). Thus, acidic residues upstream of the dileucine motif appear to be important for the localization of VMAT2, as well as VAChT.

VMATs localize almost exclusively to LDCVs in PC12 cells, and therefore cofractionate to a high degree with SGII in the heavy fractions of sucrose equilibrium sucrose gradients (Liu et al., 1994). Increased localization of the VAChT mutant S480E to heavy fractions suggests that neutralization of Glu-478 and Glu-479 might conversely reduce the localization of VMAT2 to LDCVs. HA-tagged VMAT2 cofractionates nearly identically with SGII, consistent with its localization to LDCVs (Fig. 8 A). In contrast, the E478A/E479A mutant cofractionates with SgII to a lesser extent, and the profile of VMAT2 immunoreactivity across the gradient differs greatly from that of the LDCV marker (Fig. 8 B). Since wild-type VMAT2 resides almost entirely on LDCVs, these results indicate that neutralization of Glu-478 and -479 reduces the proportion of VMAT2 expressed on LDCVs. Acidic residues upstream of the dileucine motif in VMAT2 thus influence sorting of the transporter to this population of regulated secretory vesicles.

S480E Increases VAChT Sorting to LDCVs

Replacement of Ser-480 to mimic phosphorylation redistributes VAChT to the tips of processes in PC12 cells, and to heavier fractions in density gradients. To determine whether the S480E mutation specifically increases localization of VAChT to LDCVs, we have used additional membrane fractionation and immunoelectron microscopy to assess the localization of the S480E mutant to LDCVs. A two-step fractionation procedure involving velocity sedimentation, followed by equilibrium sedimentation (Stinchcombe and Huttner, 1994), separates LDCVs from other membranes of similar size and density. A small percentage of wild-type (Liu et al., 1994) and HA-tagged VAChT (~4.5%) resides on LDCVs (Fig. 9). However, mutations at Ser-480 change the amount of HA-tagged VAChT in LDCV fractions relative to the amount of transporter in starting material loaded onto the first velocity gradient (Fig. 9). The S480A mutant localizes to LDCVs to a slightly lesser extent (~3.4%), and the S480E mutation increases expression on LDCVs to ~10.6%, 2.3-fold more than wild-type, and about threefold more than the S480A mutant. The low proportion of VAChT on LDCVs, even in the case of the S480E mutant may reflect the inefficiency of the two-step procedure, which results in more highly purified LDCVs at the expense of yield.

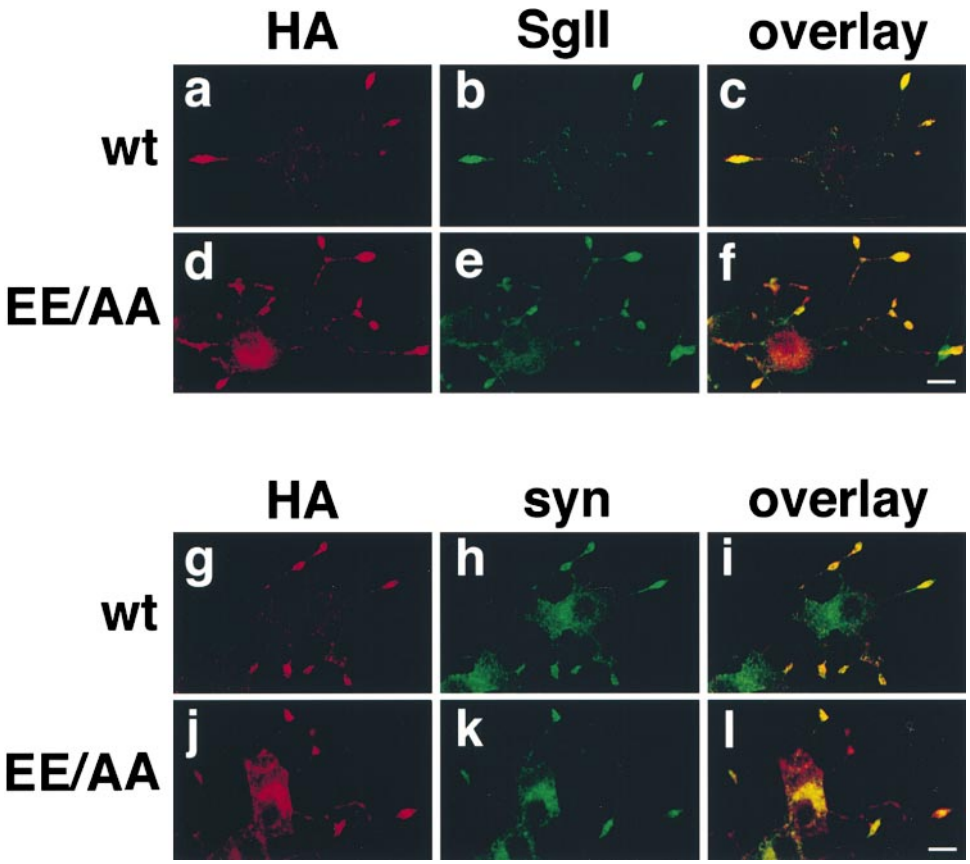

Figure 7. Neutralization of glutamates-478 and -479 in VMAT2. To eliminate the negative charge upstream of the dileucine motif in VMAT2, Glu-478 and -479 were replaced by alanine. PC12 cells stably expressing wild-type VMAT2 and the E478A/E479A mutant (EE/AA) were double-stained with a mouse mAb to the HA epitope (a, d, g, and j) and either a rabbit polyclonal antiserum to SgII (b and e), or a rabbit antibody to synaptophysin (syn; h and k). Secondary anti-mouse antibodies conjugated to Cy3 (a, d, g, and j) or anti-rabbit antibodies conjugated to Cy5 (b, e, h, and k) were used to visualize the proteins, and the cells were examined by confocal microscopy. The overlay of Cy3 and Cy5 images are shown in c, f, i, and l. Wild-type VMAT2 colocalizes with both SgII and synaptophysin at the tips of cell processes, but does not colocalize with synaptophysin at cell bodies. In contrast, the EE/AA mutant resides at high levels in cell bodies and exhibits greater colocalization with synaptophysin than wild-type VMAT2. Bars, 10 μm.

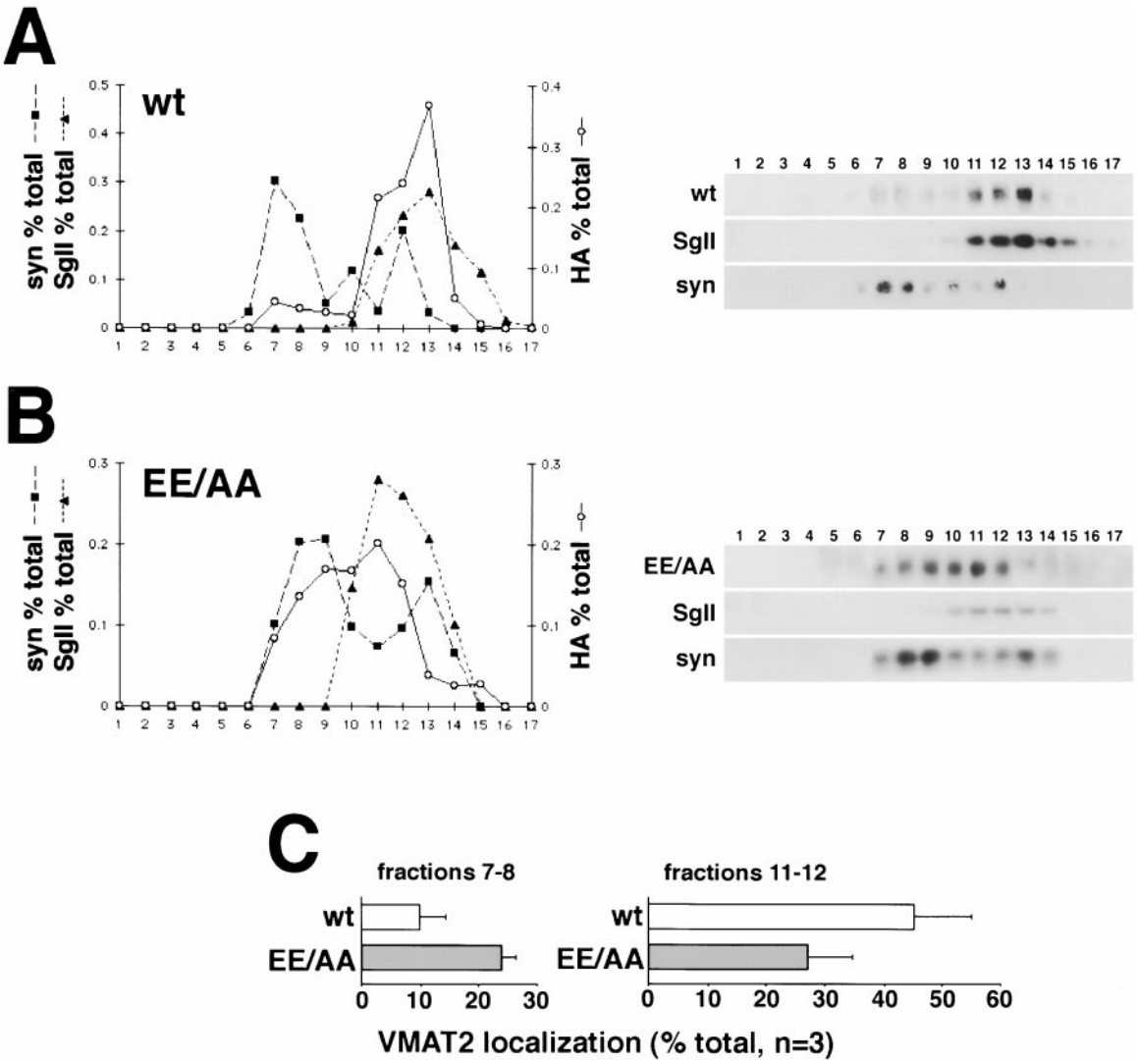

Figure 8. The E478A/E479A mutation redistributes VMAT2 away from LDCVs. PNSs of PC12 cells stably expressing HA-tagged wild-type VMAT2 and the E478A/E479A (EE/AA) mutant were separated by equilibrium sedimentation through 0.6–1.6 M sucrose. The fractions were analyzed by Western blot using a monoclonal HA antibody for VMAT2 (top of immunoblots in A and B), a polyclonal antibody to SgII (middle), and an mAb to synaptophysin (bottom). The immunoblots shown in A and B were digitized, quantified, and the amounts of HA-tagged VMAT2, synaptophysin, and SgII was expressed as a percentage of total immunoreactivity. Wild-type VMAT2 cofractionates more strongly with SgII than with synaptophysin. In contrast, the EE/AA mutation shifts VMAT2 into lighter membrane fractions. D, The proportion of VMAT2 localized to light fractions 6–8 (left) or heavy fractions 11–12 was expressed as a percentage of total VMAT2 immunoreactivity across the gradients, using the data shown in A–C and two additional independently isolated cell lines for each mutant. The bar graph shows the mean ± standard error ($n = 3$).

Nonetheless, the S480A mutation modestly reduces, and the S480E mutation clearly increases, the expression of VAChT on LDCVs, indicating that an acidic residue at position 480 increases localization of VAChT to LDCVs, and suggesting that a negatively charged phosphoserine at this position in wild-type VAChT may similarly direct the transporter to LDCVs.

The subcellular location of wild-type VAChT, as well as the S480A and S480E mutants, was analyzed in more detail by immunogold labeling of ultrathin cryosections (Fig. 10). LDCVs in PC12 cells appear in cryosections as 75–125-nm diam compartments with an electrodense core (Fig. 10 E) that labels for SgII (not shown). In agreement with previous observations, wild-type VAChT localizes to LDCVs, as well as numerous small vesicular profiles found in the area near the Golgi complex (Fig. 10 A), near endosomes (Fig. 10 B), or on membranes dispersed throughout the cytoplasm (Weihe et al., 1996; Liu and Edwards, 1997a; Fig. 10 C). Label was also found directly over the Golgi complex, plasma membrane, and endosomes. Double-labeling shows that VAChT and synaptophysin colocalize to a high degree in the small vesicular profiles (Fig. 10 C) which largely represent the SLMVs of PC12 cells (de Wit et al., 1999). VAChT appears in early endosomes as well, characterized by a limited number of internal membranes (Fig. 10 B), but is absent from densely filled late

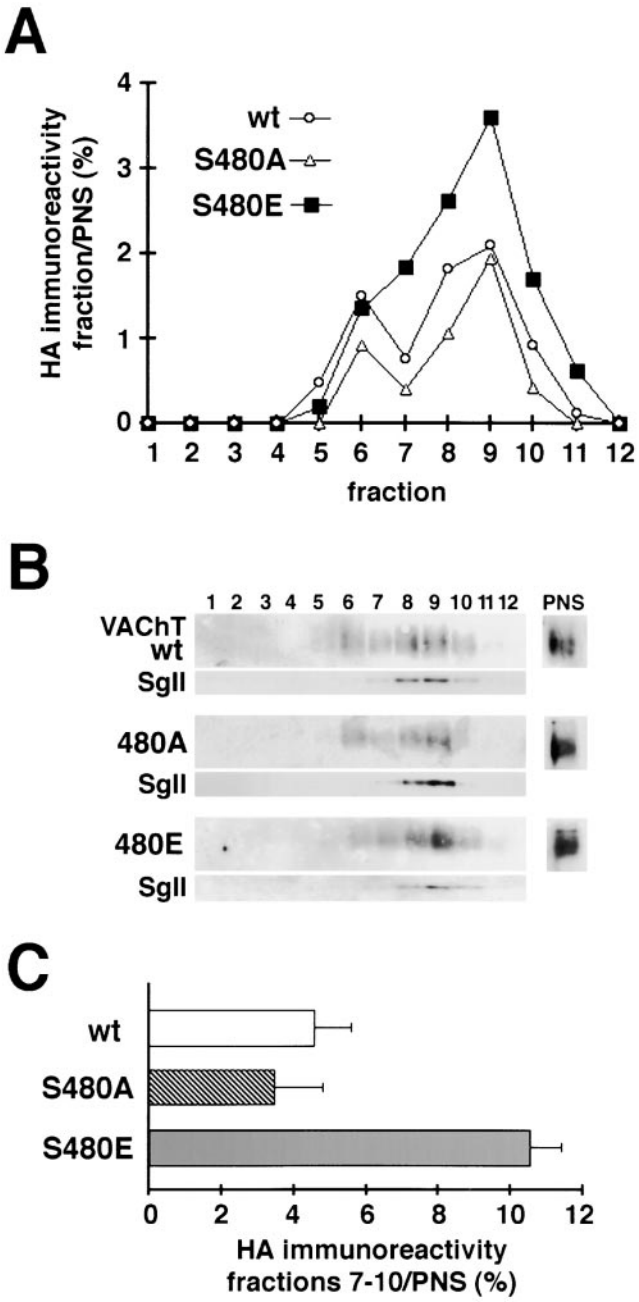

Figure 9. Localization of wild-type and mutant VAChT to LDCVs. PNSs of PC12 cells stably expressing wild-type VAChT (wt), and S480A and S480E mutants preloaded with [^{3}H]serotonin were separated on a sucrose velocity gradient, the peak LDCV fractions determined by scintillation counting, pooled, and separated again by equilibrium sedimentation through sucrose. The fractions were immunoblotted with an mAb to the HA tag and the amount of HA immunoreactivity in each fraction of the second gradient was quantified and expressed as a proportion of immunoreactivity in the starting material (PNS) loaded onto the first gradient (A). The peak of HA immunoreactivity on the second density gradient coincides with that of the LDCV marker SgII (B), and with the peak of [^{3}H]serotonin (not shown). The average ± SEM was determined from two independently isolated cell lines for each mutant (C). S480E localizes to LDCVs ~2.3-fold and threefold better than wild-type VAChT and the S480A mutant, respectively.

Table I. Distribution of S480A and S480E VAChT to Secretory Vesicles

A. Localization of gold particles to LDCVs

Mutant	LDCV/total
	%
S480A	17.5 ± 3
S480E	29.4 ± 2.7

B. Relative distribution of particles to LDCVs versus SLMVs

Mutant	LDCVs/(LDCVs ± SLMVs)
	%
S480A	40.3 ± 1.6
S480E	55.9 ± 2.5

In immunogold-labeled ultrathin cryosections, the number of gold particles representing VAChT mutants S480A and S480E, over LDCVs, SLMVs, and other compartments was counted blindly. The percentage of VAChT localized to LDCVs relative to the total counted particles (A) and the percentage of gold particles found over either LDCVs relative to the sum of particles over LDCVs plus SLMVs (B) are indicated in the table.

endosomes and lysosomes (Fig. 10 A). Notably, the limiting membrane of the vacuolar part of early endosomes (also known as the sorting endosome) contains relatively little VAChT label, whereas dense labeling appears over surrounding vesicles. A similar steady-state distribution over early endosomes has previously been shown for synaptophysin (Clift-O'Grady et al., 1990; Cameron et al., 1991; Regnier-Vigouroux et al., 1991) and implies rapid sorting of proteins into recycling vesicles.

The S480A and S480E mutants label the same compartments as wild-type VAChT (Fig. 10, D and E), but with different relative distributions. Of all the gold particles present in a section, 17.5% S480A and 29.4% S480E appear over the membrane of LDCVs (Table I). In addition, when the distribution of gold particles between only LDCVs and SLMVs was quantitated, 40% S480A and 56% S480E were found over LDCVs (Table I). Consistent with the immunofluorescence and biochemical fractionation, immunoelectron microscopy thus provides quantitative evidence for the increased localization of S480E to LDCVs.

Discussion

In addition to differences in their contents, subcellular location and mode of release, LDCVs and SVs differ in their biogenesis (Bauerfeind and Huttner, 1993; Kelly, 1993; Martin, 1994). Electron microscopic observations have indicated that LDCVs bud directly from the trans-Golgi network (TGN; Farquhar et al., 1978; Tooze and Tooze, 1986; Orci et al., 1987). After a maturation process that involves the removal of proteins destined for other intracellular membranes (Tooze et al., 1991; Klumperman et al., 1998), LDCVs undergo regulated exocytosis. In contrast, SVs do not form at the TGN. Rather, proteins destined for SVs sort to constitutive secretory vesicles at the TGN, arrive at the plasma membrane in the absence of stimulation, and enter SVs only after recycling from the cell surface (Clift-O'Grady et al., 1990; Cameron et al., 1991; Regnier-Vigouroux et al., 1991). However, relatively little is known about the signals that sort proteins to either LDCVs or SVs (Grote et al., 1995; Haucke and De Camilli, 1999).

Previous studies of protein sorting to LDCVs have focused on their soluble contents. Although recent work has

implicated the processing enzyme carboxypeptidase E in sorting to LDCVs (Cool et al., 1997), most neural peptides sort into LDCVs as a result of aggregation under the particular redox and pH conditions of nascent LDCVs (Chanat and Huttner, 1991; Rindler, 1998). Thus, the soluble cargo of LDCVs are not thought to contain a specific sorting sequence, but rather to enter the regulated secretory pathway as a result of their general biophysical properties. In contrast, integral membrane proteins of the LDCV have the potential to interact directly with sorting machinery through their cytoplasmic domains which presumably contain specific sorting signals.

Most of the integral membrane proteins present on LDCVs also occur at substantial levels on SVs. These include the vSNARE proteins involved in vesicle docking and fusion (Schmidle et al., 1991; Glenn and Burgoyne, 1996), as well as certain isoforms of the calcium sensor synaptotagmin (Schmidle et al., 1991; Walch-Solimena et al., 1993). Heterologous expression in neuroendocrine cells of the endothelial protein P-selectin also confers expression on both LDCVs and SVs (Norcott et al., 1996). In contrast, VMATs localize preferentially to LDCVs in PC12 cells, indicating that they sort more specifically to the regulated secretory pathway (Liu et al., 1994). The closely related VAChT also occurs on LDCVs, but at a much lower level than the VMATs (Liu and Edwards, 1997a; Varoqui and Erickson, 1998). VAChT preferentially localizes to lighter membranes, including endosomes and SLMVs in PC12 cells, indicating substantial differences in trafficking from the VMATs. Recent observations also indicate that the differential trafficking of the transporters depends on signals contained in their cytoplasmic, COOH-terminal domains (Tan et al., 1998; Varoqui and Erickson, 1998).

Using a combination of immunofluorescence, biochemical fractionation, and immunoelectron microscopy, we now show that mutation of Ser-480 regulates membrane trafficking of VAChT to LDCVs. By immunofluorescence, the distribution of wild-type and the S480A mutant protein resembles that of synaptophysin. In contrast, the localization of S480E differs from wild-type VAChT and S480A, and more closely resembles that of the LDCV marker SGII. Equilibrium sedimentation through sucrose also reveals a larger proportion of S480E than wild-type VAChT in heavy fractions, comigrating with LDCVs.

Mutation of acidic residues upstream of the dileucine motif in VMAT2 (Glu-478 and -479) also alters transporter localization. However, unlike VAChT, wild-type VMATs localize almost exclusively to LDCVs (Liu et al., 1994). The effect of VAChT mutations at Ser-480 suggest that neutralization of glutamate residues upstream of the dileucine motif in VMAT2 might reduce localization to LDCVs. Indeed, immunofluorescence and sucrose equilibrium gradients show that replacement of Glu-478 and -479 by alanine partially redistributes VMAT2 to lighter membranes and away from LDCVs. The E478/479A mutation does not eliminate localization of VMAT2 to LDCVs, and additional signals may contribute to the sorting of VMAT2. The results nonetheless suggest that acidic residues upstream of a dileucine motif are involved in the trafficking of VMAT2 to regulated secretory vesicles.

In addition, two-step fractionation shows that the S480E mutation increases localization of VAChT to LDCVs relative to wild-type protein and the S480A mutant. Quantitative immunoelectron microscopy further confirms the increased expression of S480E on LDCVs, although the difference from S480A appears less marked than the threefold increase observed by the two-step fractionation procedure. Losses of starting material during fractionation may have amplified slightly the difference in localization between S480A and S480E. Nonetheless, analysis of the mutants strongly suggests that a negative charge five residues upstream of the dileucine motif increases the sorting of VAChT to LDCVs.

Both gradient fractionation and immunoisolation indicate a corresponding decrease in the sorting of S480E to synaptophysin containing vesicles. However, synaptophysin localizes to both endosomes and SLMVs in PC12 cells (Clift-O'Grady et al., 1990; Cameron et al., 1991). We therefore performed velocity gradient fractionation to specifically determine the effect of S480E on SLMVs. Since the S480E mutant sorts to SLMVs in proportions similar to wild-type and S480A, the negative charge upstream of the dileucine motif may not influence sorting to SLMVs, at least in PC12 cells. In neurons, however, synaptophysin localizes almost exclusively to SVs, and the dominant pathway of SV biogenesis is likely to differ from that used in PC12 cells (Shi et al., 1998), leaving open the possibility that phosphorylation of Ser-480 influences the localization to SVs in neurons.

Very few, if any, other signals responsible for localization to LDCVs have previously been identified. The protein P-selectin, which localizes to secretory granules in endothelial cells and to LDCVs after heterologous expression in PC12 cells (Norcott et al., 1996), has a sequence at its cytoplasmic COOH terminus (KDDG) that resembles the sequence of basic and acidic residues in the VMATs and VAChT. However, unlike the VMATs and VAChT, selectin does not contain a dileucine-like motif flanking the charged residues. Indeed, replacement of the KDDG sequence in P-selectin by four alanines does not apparently reduce targeting to LDCVs, and other signals in P-selectin mediate localization to secretory vesicles (Blagoveshchenskaya et al., 1999).

The signals that direct neurotransmitter transporters to secretory vesicles presumably interact with a cytoplasmic sorting machinery that may include clathrin adaptor proteins, such as AP-1 and -2, and the related AP-3 and AP-4 (Bonifacino and Dell'Angelica, 1999). Dileucine motifs are generally considered to interact directly with the β subunit of adaptors (Rapoport et al., 1998). However, acidic residues and phosphorylation sites upstream of dileucine signals have also been implicated in the internalization of plasma membrane proteins. These residues may bind directly to the adaptors, or they may modulate adaptor binding indirectly (Dietrich et al., 1997). Regardless of the precise mechanism, the spacing between these upstream residues and the leucines appears important and in some cases, the upstream acidic residues and the two leucines function as a single motif (Dietrich et al., 1997). These observations suggest that the acidic residues upstream of the dileucine motif in VAChT and the VMATs act in concert with the two leucines, or modulate their ability to interact with the cytoplasmic sorting machinery.

The signal we have identified could act at several sites in

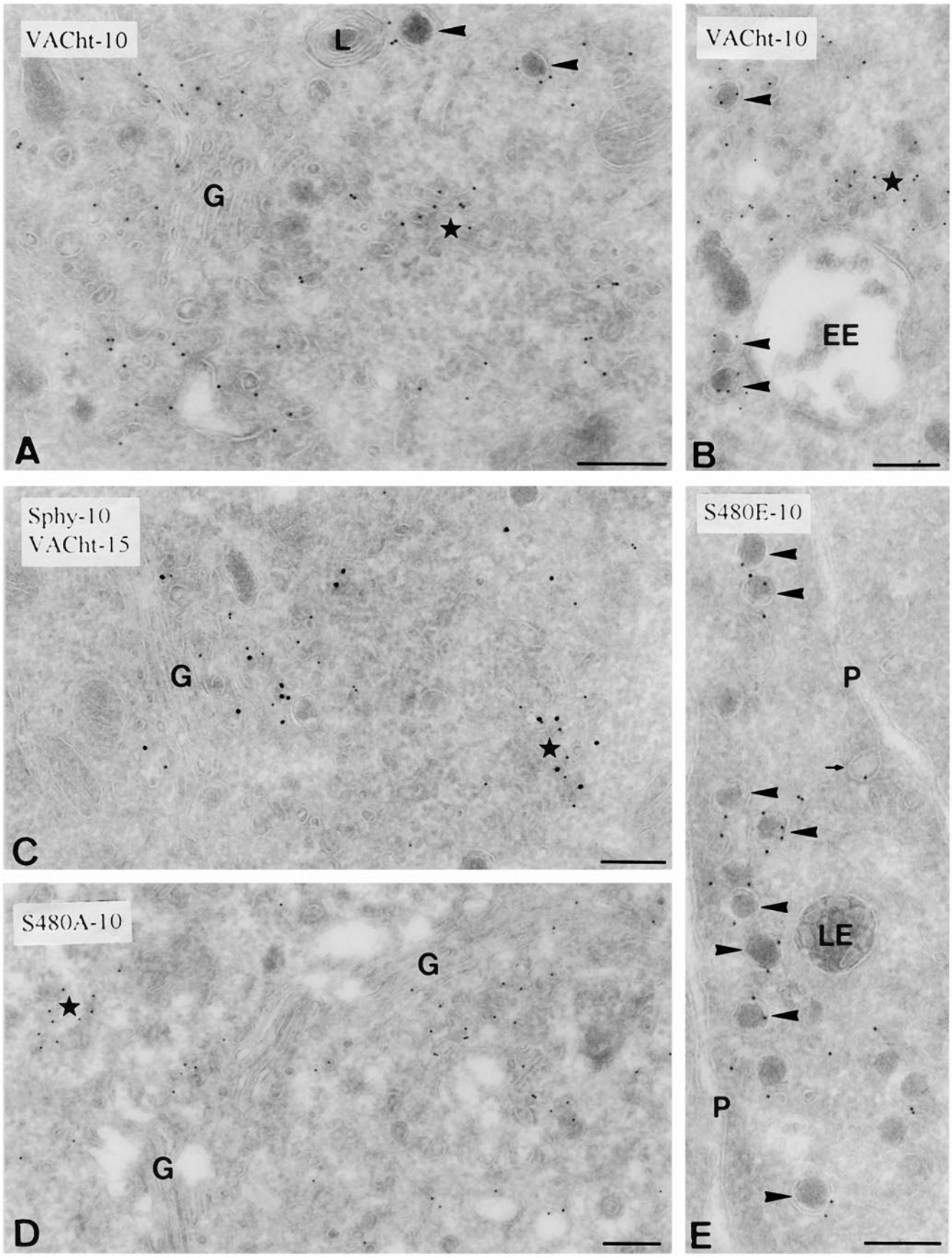

the cell to affect localization to LDCVs. First, it could act in the TGN to direct the vesicular transporters toward the regulated secretory pathway (LDCVs) and away from the constitutive secretory pathway. Second, it could influence retrieval from immature LDCVs. Immature LDCVs contain resident TGN proteins, such as furin (Dittie et al., 1997), and lysosomal proteins, such as cathepsin B (Kuliawat et al., 1997). Maturation of the LDCVs involves the removal of these proteins by an AP-1– and clathrin-dependent mechanism (Dittie et al., 1996; Klumperman et al., 1998), and phosphorylation of an acidic patch by casein kinase II promotes retrieval by recruiting a novel cytosolic protein (Wan et al., 1998). Acidic residues upstream of the dileucine motifs present in the neurotransmitter transporters might thus act by suppressing retrieval from immature LDCVs, thereby increasing expression on mature LDCVs. Third, the dileucine-based signals may influence the recycling of VAChT and the VMATs from the cell surface after exocytosis. Upstream acidic residues may suppress local recycling to endosomes or synaptic vesicles and so direct the proteins to the TGN and then to LDCVs. The precise membrane trafficking step(s) affected by acidic residues upstream of the dileucine motif in vesicular transporters remain to be determined. However, the role of the dileucine motif in internalization from the plasma membrane (Tan et al., 1998) indicates that the dileucine motif itself functions at multiple trafficking steps, with the upstream acidic residues perhaps required for a subset of these events.

Phosphorylation of Ser-480 in VAChT provides a negative charge similar to the glutamate present at this position in the VMATs. Metabolic labeling in unstimulated PC12 cells indicates that constitutive phosphorylation may contribute to the localization of wild-type VAChT. However, since wild-type VAChT localizes to LDCVs in amounts similar to the S480A mutant, constitutive phosphorylation presumably occurs at low levels. Activation of PKC increases VAChT phosphorylation, and may increase the localization of the transporter to LDCVs.

The localization of VAChT to LDCVs in PC12 cells has relevance for the site of ACh storage in vivo. Although SVs are generally considered to store and release from ACh at the neuromuscular junction and in brain (Gilmor et al., 1996; Weihe et al., 1996), ACh also appears in vesicles similar to, or identical to LDCVs by biochemical fractionation (Lundberg et al., 1981; Agoston and Whittaker, 1989). In addition, light microscopic analysis of brain sections shows a distribution for VAChT very similar to that of VMAT2, with strong staining of cell bodies and dendrites not observed with other synaptic vesicle proteins, including the vesicular GABA transporter (Schafer et al., 1995; Gilmor et al., 1996; Chaudhry et al., 1998). Thus, the regulation of VAChT trafficking by phosphorylation of Ser-480 may also influence the distribution of the protein in vivo.

A change in the trafficking of VAChT has the potential to affect transmitter release. A number of observations indicate that vesicular transport activity influences the amount of transmitter released per vesicle, or quantal size. Mice heterozygous for a disruption of the VMAT2 gene show dramatically reduced storage and release of dopamine and serotonin (Fon et al., 1997). VMAT2 heterozygotes (±) also show behavioral differences from wild-type animals (Takahashi et al., 1997; Wang et al., 1997). In addition, overexpression of rat VAChT in *Xenopus laevis* embryos generates larger postsynaptic quantal events in cocultured myocytes (Song et al., 1997). Alterations in the localization of VAChT to LDCVs (or SVs) may therefore affect the amount of transmitter stored and released by these vesicle populations.

The observations have relevance for certain forms of neural plasticity. The neuromuscular junction exhibit considerable variation in quantal size and the mechanism(s) appears to be presynaptic (Van der Kloot, 1990; Williams, 1997). Drugs that inhibit vesicular ACh transport block the regulation, implicating VAChT in the mechanism, and protein phosphorylation also appears to be involved (Van Der Kloot and Molgo, 1994). In the central nervous system, PKC also modulates ACh release (Tanaka et al., 1986; Allgaier et al., 1988). Activation of PKC increases VAChT phosphorylation, as well as ACh release in hippocampal synaptosomes, and the changes in transmitter release require VAChT function (Barbosa et al., 1997). The phosphorylation of VAChT by PKC at Ser-480 may thus contribute to multiple forms of neural plasticity by influencing the distribution of the transport protein on neurosecretory vesicles. The difference that we have observed between trafficking of S480A and S480E mutants indicates the potential for phosphorylation at Ser-480 to influence quantal size. The magnitude of the differences in localization resembles the magnitude changes in quantal size observed for other forms of synaptic plasticity (Malenka and Nicoll, 1993). Further, the localization of VAChT to LDCVs and its regulation by phosphorylation of Ser-480 may specifically contribute to the giant endplate potentials observed at the neuromuscular junction (Van der Kloot, 1990), and help to account for this poorly understood mode of ACh release.

Figure 10. Immunoelectron microscopy of PC12 cells expressing wild-type and mutant VAChT. Immunogold-labeled cryosections from PC12 cells expressing wild-type VAChT (A–C), S480A (D), or S480E (E) were examined by EM. Labeled LDCVs are indicated by arrowheads, whereas VAChT-positive small vesicular profiles are indicated with an asterisk. A, VAChT (10-nm gold) is found in the Golgi complex (G), as well as many neighboring vesicles (asterisk). LDCVs (arrowheads) are positive, but no label is found on lysosomes (L). B, Example of VAChT label (10-nm gold) in small vesicles close to an early endosomal vacuole (EE). C, Double immunogold-labeling shows that synaptophysin (Sphy, 10-nm gold) colocalizes to a considerable extent with VAChT (15-nm gold) in small vesicular profiles (asterisk). D, S480A (10-nm gold) localizes preferentially to small vesicles. E, By contrast, S480E (10-nm gold) is found preferentially in LDCVs. The small arrow points to a clathrin-coated pit at the plasma membrane (P). LE, late endosome. Bars, 200 nm.

We thank the members of the Edwards lab for thoughtful discussion, and Victor Faundez, Jack Roos, and Ted Fon for helpful comments on the text. Rene Scriwanek and Tom van Rijn are acknowledged for the preparation of electron micrographs.

This work was supported by a Postdoctoral Fellowship for Physicians from the Howard Hughes Medical Institute (to D.E. Krantz), a National Science Foundation Graduate Research Fellowship (to R.I. Wilson), a Young Investigator Award from the National Alliance for Research on Schizophrenia and Affective Disorders (NARSAD; to Y. Liu), the National Parkinson Foundation (Y. Liu), and the National Institutes of Mental Health (P.K. Tan and R.H. Edwards) and Drug Abuse (R.H. Edwards).

Submitted: 24 September 1999
Revised: 6 March 2000
Accepted: 6 March 2000

References

Agoston, D.V., and V.P. Whittaker. 1989. Characterization, by size, density, osmotic fragility, and immunoaffinity, of acetylcholine- and vasoactive intestinal polypeptide-containing storage particles from neurones of the guinea-pig. *J. Neurochem.* 52:1474–1480.

Allgaier, C., B. Daschmann, H. Huang, and G. Hertting. 1988. Protein kinase C and presynaptic modulation of acetylcholine release in rabbit hippocampus. *Br. J. Pharmacol.* 93:525–534.

Barbosa, J., Jr., A.D. Clarizia, M.V. Gomez, M.A. Romano-Silva, V.F. Prado, and M.A.M. Prado. 1997. Effect of protein kinase C activation on the release of [^{3}H] acetylcholine in the presence of vesamicol. *J. Neurochem.* 69:2608–2611.

Bauerfeind, R., and W.B. Huttner. 1993. Biogenesis of constitutive secretory vesicles, secretory granules and synaptic vesicles. *Curr. Opin. Cell Biol.* 5:628–635.

Blagoveshchenskaya, A.D., E.W. Hewitt, and D.F. Cutler. 1999. A complex web of signal-dependent trafficking underlies the triorganellar distribution of P-selectin in neuroendocrine PC12 cells. *J. Cell Biol.* 145:1419–1433.

Bonifacino, J.S., and E.C. Dell'Angelica. 1999. Molecular bases for the recognition of tyrosine-based sorting signals. *J. Cell Biol.* 145:923–926.

Boyle, W.J., P. van der Geer, and T. Hunter. 1991. Phosphopeptide mapping and phosphoamino acid analysis by two-dimensional separation on thin-layer cellulose plates. *Methods Enzymol.* 201:110–149.

Bruns, D., and R. Jahn. 1995. Real-time measurement of transmitter release from single synaptic vesicles. *Nature.* 377:62–65.

Calakos, N., and R.H. Scheller. 1996. Synaptic vesicle biogenesis, docking, and fusion: a molecular description. *Physiol. Rev.* 76:1–29.

Cameron, P.L., T.C. Sudhof, R. Jahn, and P. de Camilli. 1991. Colocalization of synaptophysin with transferrin receptors: implications for synaptic vesicle biogenesis. *J. Cell Biol.* 115:151–164.

Chanat, E., and W.B. Huttner. 1991. Milieu-induced, selective aggregation of regulated secretory proteins in the trans-Golgi network. *J. Cell Biol.* 115: 1505–1519.

Chaudhry, F.A., R.J. Reimer, E.E. Bellocchio, N.C. Danbolt, K.K. Osen, R.H. Edwards, and J. Storm-Mathisen. 1998. The vesicular GABA transporter, VGAT, localizes to synaptic vesicles in sets of glycinergic as well as GABAergic neurons. *J. Neurosci.* 18:9733–9750.

Chijiwa, T., A. Mishima, M. Hagiwara, M. Sano, K. Hayashi, T. Inoue, K. Naito, T. Toshioka, and H. Hidaka. 1990. Inhibition of forskolin-induced neurite outgrowth and protein phosphorylation by a newly synthesized selective inhibitor of cyclic AMP-dependent protein kinase, N-[2-(p-bromocinnamylamino)ethyl]-5-isoquinolinesulfonamide (H-89), of PC12D pheochromocytoma cells. *J. Biol. Chem.* 265:5267–5272.

Clift-O'Grady, L., A.D. Linstedt, A.W. Lowe, E. Grote, and R.B. Kelly. 1990. Biogenesis of synaptic vesicle-like structures in a pheochromocytoma cell line PC12. *J. Cell Biol.* 110:1693–1703.

Cool, D.R., E. Normant, F. Shen, H.C. Chen, L. Pannell, Y. Zhang, and Y.P. Loh. 1997. Carboxypeptidase E is a regulated secretory pathway sorting receptor: genetic obliteration leads to endocrine disorders in Cpe(fat) mice. *Cell.* 88:73–83.

Davidson, H.W., C.H. McGowan, and W.E. Balch. 1992. Evidence for the regulation of exocytotic transport by protein phosphorylation. *J. Cell Biol.* 116: 1343–1355.

De Camilli, P., and R. Jahn. 1990. Pathways to regulated exocytosis in neurons. *Ann. Rev. Physiol.* 52:625–645.

De Mattheis, M.A., G. Santini, R.A. Kahn, G. Di Tullio, and A. Luini. 1993. Receptor and protein kinase C-mediated regulation of ARF binding to the Golgi complex. *Nature.* 364:818–821.

de Wit, H., Y. Lichtenstein, H.J. Geuze, R.B. Kelly, P. van der Sluijs, and J. Klumperman. 1999. Synaptic vesicles form by budding from tubular extensions of sorting endosomes in PC12 cells. *Mol. Biol. Cell.* 10:4163–4176.

Dietrich, J., X. Hou, A.M. Wegener, and C. Geisler. 1994. CD3 gamma contains a phosphoserine-dependent di-leucine motif involved in down-regulation of the T cell receptor. *EMBO (Eur. Mol. Biol. Organ.) J.* 13:2156–2166.

Dietrich, J., J. Kastrup, B.L. Nielsen, N. Odum, and C. Geisler. 1997. Regulation and function of the CD3 gamma DXXXLL motif: a binding site for adaptor protein-1 and adaptor protein-2 in vitro. *J. Cell Biol.* 138:271–281.

Dittie, A.S., N. Hajibagheri, and S.A. Tooze. 1996. The AP-1 adaptor complex binds to immature secretory granules from PC12 cells, and is regulated by ADP-ribosylation factor. *J. Cell Biol.* 132:523–536.

Dittie, A.S., L. Thomas, G. Thomas, and S.A. Tooze. 1997. Interaction of furin in immature secretory granules from neuroendocrine cells with the AP-1 adaptor complex is modulated by casein kinase II. *EMBO (Eur. Mol. Biol. Organ.) J.* 16:4859–4870.

Erickson, J.D., and L.E. Eiden. 1993. Functional identification and molecular cloning of a human brain vesicle monoamine transporter. *J. Neurochem.* 61: 2314–2317.

Erickson, J.D., H. Varoqui, M.D. Schafer, W. Modi, M.F. Diebler, E. Weihe, J. Rand, L.E. Eiden, T.I. Bonner, and T.B. Usdin. 1994. Functional identification of a vesicular acetylcholine transporter and its expression from a "cholinergic" gene locus. *J. Biol. Chem.* 269:21929–21932.

Erickson, J.D., M.K. Schafer, T.I. Bonner, L.E. Eiden, and E. Weihe. 1996. Distinct pharmacological properties and distribution in neurons and endocrine cells of two isoforms of the human vesicular monoamine transporter. *Proc. Natl. Acad. Sci. USA.* 93:5166–5171.

Farquhar, M.G., J.J. Reid, and L.W. Daniell. 1978. Intracellular transport and packaging of prolactin: a quantitative electron microscope autoradiographic study of mammotrophs dissociated from rat pituitaries. *Endocrinology.* 102: 296–311.

Finn, J.P., III, and R.H. Edwards. 1998. Multiple residues contribute independently to differences in ligand recognition between vesicular monoamine transporters 1 and 2. *J. Biol. Chem.* 273:3943–3947.

Fon, E.A., E.N. Pothos, B.-C. Sun, N. Kileen, D. Sulzer, and R.H. Edwards. 1997. Vesicular transport regulates monoamine storage and release but is not essential for amphetamine action. *Neuron.* 19:1271–1283.

Frize, E.D. 1954. Mental depression in hypertensive patients treated for long periods with high doses of reserpine. *N. Engl. J. Med.* 251:1006–1008.

Gilmor, M.L., N.R. Nash, A. Roghani, R.H. Edwards, H. Yi, S.M. Hersch, and A.I. Levey. 1996. Expression of the putative vesicular acetylcholine transporter in rat brain and localization in cholinergic synaptic vesicles. *J. Neurosci.* 16:2179–2190.

Glenn, D.E., and R.D. Burgoyne. 1996. Botulinum neurotoxin light chains inhibit both $Ca^{(2+)}$-induced and GTP analogue-induced catecholamine release from permeabilised adrenal chromaffin cells. *FEBS Lett.* 386:137–140.

Greene, L.A., and A.S. Tischler. 1976. Establishment of a noradrenergic clonal line of rat adrenal pheochromocytoma cells which respond to nerve growth factor. *Proc. Natl. Acad. Sci. USA.* 73:2424–2428.

Grote, E., M.K. Hao, M.K. Bennett, and R.B. Kelly. 1995. A targeting signal in VAMP regulating transport to synaptic vesicles. *Cell.* 81:581–589.

Haucke, V., and P. De Camilli. 1999. AP-2 recruitment to synaptotagmin stimulated by tyrosine-based endocytic motifs. *Science.* 285:1268–1271.

Hidaka, H., M. Inagaki, S. Kawamoto, and Y. Sasaki. 1984. Isoquinolinesulfonamides, novel and potent inhibitors of cyclic nucleotide dependent protein kinase and protein kinase C. *Biochemistry.* 23:5036–5041.

Kelly, R.B. 1993. Storage and release of neurotransmitters. *Cell.* 72Suppl:43–53.

Klumperman, J., R. Kuliawat, J.M. Griffith, H.J. Geuze, and P. Arvan. 1998. Mannose-6-phosphate receptors are sorted from immature secretory vesicles via adaptor protein AP-1, clathrin and syntaxin 6-positive vesicles. *J. Biol. Chem.* 1441:359–371.

Krantz, D.E., D. Peter, Y. Liu, and R.H. Edwards. 1997. Phosphorylation of a vesicular monoamine transporter by casein kinase II. *J. Biol. Chem.* 272: 6752–6759.

Krejci, E., B. Gasnier, D. Botton, M.F. Isambert, C. Sagne, J. Gagnon, J. Massoulie, and J.P. Henry. 1993. Expression and regulation of the bovine vesicular monoamine transporter gene. *FEBS Lett.* 335:27–32.

Kuliawat, R., J. Klumperman, T. Ludwig, and P. Arvan. 1997. Differential sorting of lysosomal enzymes out of the regulated secretory pathway in pancreatic beta-cells. *J. Cell Biol.* 137:595–608.

Kunkel, T.A., K. Bebenek, and J. McClary. 1991. Efficient site-directed mutagenesis using uracil-containing DNA. *Methods Enzymol.* 204:125–139.

Liou, W., H.J. Geuze, and J.W. Slot. 1996. Improved structural integrity of cryosections for immunogold labeling. *Histochem. Cell. Biol.* 106:41–58.

Liu, Y., and R.H. Edwards. 1997a. Differential localization of vesicular acetylcholine and monoamine transporters in PC12 cells but not CHO cells. *J. Cell Biol.* 139:907–916.

Liu, Y., and R.H. Edwards. 1997b. The role of vesicular transport proteins in synaptic transmission and neural degeneration. *Annu. Rev. Neurosci.* 20: 125–156.

Liu, Y., D. Peter, A. Roghani, S. Schuldiner, G.G. Prive, D. Eisenberg, N. Brecha, and R.H. Edwards. 1992. A cDNA that supresses MPP+ toxicity encodes a vesicular amine transporter. *Cell.* 70:539–551.

Liu, Y., E.S. Schweitzer, M.J. Nirenberg, V.M. Pickel, C.J. Evans, and R.H. Edwards. 1994. Preferential localization of a vesicular monoamine transporter to dense core vesicles in PC12 cells. *J. Cell Biol.* 127:1419–1433.

Lundberg, J.M., G. Fried, J. Fahrenkrug, B. Holmstedt, T. Hokfelt, H. Lagercrantz, G. Lundgren, and A. Anggard. 1981. Subcellular fractionation of cat submandibular gland: comparative studies of the distribution of acetylcholine and vasoactive intestinal peptide (VIP). *Neurosci.* 6:1001–1010.

Malenka, R.C., and R.A. Nicoll. 1993. NMDA-receptor–dependent synaptic plasticity: multiple forms and mechanisms. *Trends Neurosci.* 16:521–527.
Martin, T.F.J. 1994. The molecular machinery for fast and slow neurosecretion. *Curr. Opin. Neurobiol.* 4:626–632.
Merickel, A., P. Rosandich, D. Peter, and R.H. Edwards. 1995. Identification of residues involved in substrate recognition by a vesicular monoamine transporter. *J. Biol. Chem.* 270:25798–25804.
Naciff, J.M., H. Misawa, and J.R. Dedman. 1997. Molecular characterization of the mouse vesicular acetylcholine transporter gene. *NeuroReport.* 8:3467–3473.
Nirenberg, M.J., Y. Liu, D. Peter, R.H. Edwards, and V.M. Pickel. 1995. The vesicular monoamine transporter-2 is present in small synaptic vesicles and preferentially localizes to large dense core vesicles in rat solitary tract nuclei. *Proc. Natl. Acad. Sci. USA.* 92:8773–8777.
Nirenberg, M.J., J. Chan, Y. Liu, R.H. Edwards, and V.M. Pickel. 1996. Ultrastructural localization of the monoamine transporter-2 in midbrain dopaminergic neurons: potential sites for somatodendritic storage and release of dopamine. *J. Neurosci.* 16:4135–4145.
Norcott, J.P., R. Solari, and D.F. Cutler. 1996. Targeting of P-selectin to two regulated secretory organelles in PC12 cells. *J. Cell Biol.* 134:1229–1240.
Orci, L., M. Ravazzola, M. Amherdt, A. Perrelet, S.K. Powell, D.L. Quinn, and H.P. Moore. 1987. The trans-most cisternae of the Golgi complex: a compartment for sorting of secretory and plasma membrane proteins. *Cell.* 51: 1039–1051.
Pearson, R.B., and B.E. Kemp. 1991. Protein kinase phosphorylation site sequences and consensus specificity motifs: tabulation. *Methods Enzymol.* 200: 62–81.
Peter, D., J. Jimenez, Y. Liu, J. Kim, and R.H. Edwards. 1994. The chromaffin granule and synaptic vesicle amine transporters differ in substrate recognition and sensitivity to inhibitors. *J. Biol. Chem.* 269:7231–7237.
Pond, L., L.A. Kuhn, L. Teyton, M.-P. Schutze, J.A. Tainer, M.R. Jackson, and P.A. Peterson. 1995. A role for acidic residues in di-leucine motif-based targeting to the endocytic pathway. *J. Biol. Chem.* 270:19989–19997.
Rapoport, I., Y.C. Chen, P. Cupers, S.E. Shoelson, and T. Kirchhausen. 1998. Dileucine-based sorting signals bind to the beta chain of AP-1 at a site distinct and regulated differently from the tyrosine-based motif-binding site. *EMBO (Eur. Mol. Biol. Organ.) J.* 17:2148–2155.
Regnier-Vigouroux, A., S.A. Tooze, and W.B. Huttner. 1991. Newly synthesized synaptophysin is transported to synaptic-like microvesicles via constitutive secretory vesicles and the plasma membrane. *EMBO (Eur. Mol. Biol. Organ.) J.* 10:3589–3601.
Rindler, M.J. 1998. Carboxypeptidase E, a peripheral membrane protein implicated in the targeting of hormones to secretory granules, co-aggregates with granule content proteins at acidic pH. *J. Biol. Chem.* 273:31180–31185.
Roghani, A., J. Feldman, S.A. Kohan, A. Shirzadi, C.B. Gundersen, N. Brecha, and R.H. Edwards. 1994. Molecular cloning of a putative vesicular transporter for acetylcholine. *Proc. Natl. Acad. Sci. USA.* 91:10620–10624.
Schafer, M.K., E. Weihe, J.D. Erickson, and L.E. Eiden. 1995. Human and monkey cholinergic neurons visualized in paraffin-embedded tissues by immunoreactivity for VAChT, the vesicular acetylcholine transporter. *J. Mol. Neurosci.* 6:225–235.
Schmidle, T., R. Weiler, C. Desnos, D. Scherman, R. Fischer-Colbrie, E. Floor, and H. Winkler. 1991. Synaptin/synaptophysin, p65 and SV2: their presence in adrenal chromaffin granules and sympathetic large dense core vesicles. *Biochim. Biophys. Acta.* 1060:251–256.
Schuldiner, S., A. Shirvan, and M. Linial. 1995. Vesicular neurotransmitter transporters: from bacteria to humans. *Physiological Rev.* 75:369–392.
Shi, G., V. Faundez, J. Roos, E.C. Dell'Angelica, and R.B. Kelly. 1998. Neuroendocrine synaptic vesicles are formed in vitro by both clathrin-dependent and clathrin-independent pathways. *J. Cell. Biol.* 143:947–955.
Shin, J., R.L. Dunbrack, Jr., S. Lee, and J.L. Strominger. 1991. Phosphorylation-dependent down-modulation of CD4 requires a specific structure within the cytoplasmic domain of CD4. *J. Biol. Chem.* 266:10658–10665.
Slot, J.W., H.J. Geuze, S. Gigengack, G.E. Lienhard, and D.E. James. 1991. Immunolocalization of the insulin regulatable glucose transporter in brown adipose tissue of the rat. *J. Cell Biol.* 113:123–135.
Smith, D.B., and K.S. Johnson. 1988. Single-step purification of polypeptides expressed in *Escherichia coli* as fusions with glutathione S-transferase. *Gene.* 67:31–40.
Song, H.-J., G.-L. Ming, E. Fon, E. Bellocchio, R.H. Edwards, and M.-M. Poo. 1997. Expression of a putative vesicular acetylcholine transporter facilitates quantal transmitter packaging. *Neuron.* 18:815–826.
Stinchcombe, J.C., and W.B. Huttner. 1994. Purification of secretory granules from PC12 cells. *In* Cell Biology: A Laboratory Handbook. Vol. 1. J.E. Celis, editor. Academic Press, San Diego. 557–566.
Sulzer, D., T.-K. Chen, Y.Y. Lau, H. Kristensen, S. Rayport, and A. Ewing. 1995. Amphetamine redistributes dopamine from synaptic vesicles to the cytosol and promotes reverse transport. *J. Neurosci.* 15:4102–4108.
Sumi, M., K. Kiuchi, T. Ishikaka, A. Ishii, M. Hagiwara, T. Nagatsu, and H. Hidaka. 1991. The newly synthesized selective Ca^{2+}/calmodulin dependent protein kinase II inhibitor KN-93 reduces dopamine contents in PC12h cells. *Biochem. Biophys. Res. Comm.* 266:968–975.
Takahashi, N., L.L. Miner, I. Sora, H. Ujike, R.S. Revay, V. Kostic, V. Jackson-Lewis, S. Przedborski, and G. Uhl. 1997. VMAT2 knockout mice: heterozygotes display reduced amphetamine-conditioned reward, enhanced amphetamine locomotion, and enhanced MPTP toxicity. *Proc. Natl. Acad. Sci. USA.* 94:9938–9943.
Tan, P.K., C. Waites, Y. Liu, D.E. Krantz, and R.H. Edwards. 1998. A leucine-based motif mediates the endocytosis of vesicular monoamine and acetylcholine transporters. *J. Biol. Chem.* 28:17351–17360.
Tanaka, C., H. Fujiwara, and Y. Fujii. 1986. Acetylcholine release from guinea pig caudate slices evoked by phorbol ester and calcium. *FEBS Lett.* 195:129–134.
Thureson-Klein, A. 1983. Exocytosis from large and small dense cored vesicles in noradrenergic nerve terminals. *Neuroscience.* 10:245–259.
Tooze, J., and S.A. Tooze. 1986. Clathrin-coated vesicular transport of secretory proteins during the formation of ACTH-containing secretory granules in AtT20 cells. *J. Cell Biol.* 103:839–850.
Tooze, S.A., T. Flatmark, J. Tooze, and W.B. Huttner. 1991. Characterization of the immature secretory granule, an intermediate in granule biogenesis. *J. Cell Biol.* 115:1491–1503.
Toullec, D., P. Pianetti, H. Coste, P. Bellevergue, T. Grand-Perret, and M. Ajakane. 1991. The bisindolylmaleimide GF 109203X is a potent and selective inhibitor of protein kinase C. *J. Biol. Chem.* 266:1577–1581.
Van der Kloot, W. 1990. The regulation of quantal size. *Progress Neurobiol.* 36: 93–130.
Van Der Kloot, W., and J. Molgo. 1994. Quantal acetylcholine release at the vertebrate neuromuscular junction. *Physiological Reviews.* 74:899–991.
Varoqui, H., and J.D. Erickson. 1997. Vesicular neurotransmitter transporters. Potential sites for the regulation of synaptic function. *Molec. Neurobiol.* 15: 165–191.
Varoqui, H., and J.D. Erickson. 1998. The cytoplasmic tail of the vesicular acetylcholine transporter contains a synaptic vesicle targeting signal. *J. Biol. Chem.* 273:9094–9098.
Walch-Solimena, C., K. Takei, K.L. Marek, K. Midyett, T.C. Sudhof, P. De Camilli, and R. Jahn. 1993. Synaptotagmin: a membrane constituent of neuropeptide-containing large dense-core vesicles. *J. Neurosci.* 13:3895–3903.
Wan, L., S.S. Molloy, L. Thomas, G. Liu, Y. Xiang, S.L. Rybak, and G. Thomas. 1998. PACS-1 defines a novel gene family of cytosolic sorting proteins required for trans-Golgi network localization. *Cell.* 94:205–216.
Wang, Y.-M., R.R. Gainetdinov, F. Fumagalli, F. Xu, S.R. Jones, C.B. Block, G.W. Miller, R.M. Wightman, and M.C. Caron. 1997. Knockout of the vesicular monoamine transporter 2 gene results in neonatal death and supersensitivity to cocaine and amphetamine. *Neuron.* 19:1285–1296.
Weihe, E., J.H. Tao-Cheng, M.K. Schafer, J.D. Erickson, and L.E. Eiden. 1996. Visualization of the vesicular acetylcholine transporter in cholinergic nerve terminals and its targeting to a specific population of small synaptic vesicles. *Proc. Natl. Acad. Sci. USA.* 93:3547–3552.
Williams, J. 1997. How does a vesicle know it is full? *Neuron.* 18:683–686.